NATIONAL ADVISORY COMMITTEE

FOR AERONAUTICS

TECHNICAL NOTE

No. 1089

HIGH-ALTITUDE FLIGHT COOLING INVESTIGATION OF A

RADIAL AIR-COOLED ENGINE

By Eugene J. Manganiello, Michael F. Valerino
and E. Barton Bell

Aircraft Engine Research Laboratory
Cleveland, Ohio

NACA

Washington
August 1946

NATIONAL ADVISORY COMMITTEE FOR AERONAUTICS

TECHNICAL NOTE NO. 1089

HIGH-ALTITUDE FLIGHT COOLING INVESTIGATION OF A

RADIAL AIR-COOLED ENGINE

By Eugene J. Manganiello, Michael F. Valerino
and E. Barton Bell

SUMMARY

An investigation of the cooling of an 18-cylinder, twin-row,
radial, air-cooled engine in a high-performance pursuit airplane
has been conducted for variable engine and flight conditions at
altitudes ranging from 5000 to 35,000 feet in order to provide a
basis for predicting high-altitude cooling performance from sea-
level or low-altitude test results.

The engine cooling data obtained are analyzed by the usual
NACA cooling-correlation method wherein cylinder head and barrel
temperatures are related to the pertinent engine and cooling-air
variables. A theoretical analysis is made of the effect on engine
cooling of the change of density of the cooling air across the
engine (the compressibility effect), which becomes of increasing
importance as altitude is increased. Good agreement was obtained
between the results of the theoretical analysis and the test data.
It was found that the use of the cooling-air exit density in the
NACA cooling-correlation equation is a sufficiently accurate approx-
imation of the compressibility effect to give satisfactory corre-
lation of the cooling data over the altitude range tested. It was
also found that a sea-level or low-altitude correlation based on
entrance density gives fairly accurate cooling predictions up to an
altitude of 20,000 feet.

INTRODUCTION

A method was developed by Pinkel (reference 1) for relating the
cylinder-wall temperatures of an air-cooled engine with operating
conditions, cooling-air temperature, and cooling-air weight flow.
Because pressure drop is a more easily measurable quantity than
weight flow and because the product of cooling-air entrance density
(taken relative to standard sea-level air density) and pressure

drop $\sigma_{en}\Delta p$ is a function of the weight flow, this product was substituted for weight flow in the correlation method. This substitution, which was made on the basis of incompressible-flow considerations, has proved satisfactory for the correlation of sea-level and low-altitude cooling data, as is evident from the results of numerous engine-cooling investigations (for example, references 2 and 3). For application to high-altitude flight, however, where the change of density of the cooling-air across the engine (compressibility effects) becomes significant, the weight flow and $\sigma_{en}\Delta p$ are not uniquely related and consequently the substitution is invalidated. Errors are therefore introduced in the prediction of high-altitude cooling from sea-level or low-altitude test results when the substitution is made.

Some theoretical and experimental investigations of the cooling problems at altitude have already been conducted. Reference 4 presents a theoretical study of the compressibility effect in relation to aircraft heat-exchanger operation and provides charts whereby, in a series of successive approximations, the compressible pressure drop corresponding to a given cooling-air weight flow, drag coefficient, and density change can be determined. A somewhat similar theoretical analysis of the compressibility effect in relation to engine cooling is given in reference 5, which provides charts for accurately determining compressible-flow cooling-air pressure drop. In addition, reference 5 indicates that the compressibility effect can be accounted for, to a good degree of accuracy, by the use of the product of pressure drop and exit density. This correlation of cooling-air weight flow with pressure drop on the basis of exit-density conditions was experimentally verified by Pratt & Whitney Aircraft (reference 6) in single-cylinder-engine tests over a range of simulated altitudes from sea level to 45,000 feet. A similar single-cylinder investigation (reference 7) conducted and reported concurrently with the subject tests further verifies the use of exit density experimentally and theoretically.

In order to obtain information on the cooling characteristics of air-cooled engines at altitude conditions and, in particular, to check present methods of extrapolating to high-altitude conditions the data obtained from sea-level or low-altitude cooling tests, a flight cooling investigation was conducted on an 18-cylinder, twin-row, radial, air-cooled engine installed in a high-performance pursuit airplane. The investigation consisted of flights at variable engine and flight operating conditions at altitudes ranging from 5000 to 35,000 feet. The cooling data obtained were correlated by the NACA method developed in reference 1 as modified to account for cooling-air compressibility effects. A theoretical analysis was

also made to check the validity of the use of cooling-air exit density in the correlation equation for approximating the compressibility effects.

TEST INSTALLATION

Airplane and power plant. - The engine cooling tests were conducted in a pursuit airplane on an 18-cylinder, twin-row, radial, air-cooled engine having a volumetric displacement of 2804 cubic inches. The compression ratio for the engine is 6.65, the spark setting 20° B.T.C., and the valve overlap 40°. The engine is equipped with a single-stage, single-speed blower, which has an impeller diameter of 11 inches and a gear ratio of 7.6:1. A turbosupercharger consisting of a single-stage impulse turbine wheel with a 13.2-inch pitch-line diameter shafted directly to a 15-inch-diameter impeller provides the supercharging required for high-altitude operation. An injection-type carburetor meters the fuel to the engine at the inlet face of the engine-stage blower. The power plant is rated as follows:

	Horse-power	Engine speed (rpm)	Altitude (ft)
Normal	1625	2550	29,000
Emergency maximum	2000	2700	27,000
Take-off	2000	2700	------

The engine power is delivered through a 2:1 reduction gear to an electrically controllable four-bladed propeller having a diameter of 12 feet 2 inches. The propeller is fitted with shank cuffs and is not provided with a spinner hub.

A photograph of the airplane used in the flight tests is presented in figure 1. Figure 2 is a schematic diagram of the power-plant installation showing the general arrangement of the internal air-ducting system and the relative positions on the airplane of the engine, the cowling, the turbosupercharger, the intercooler, and the oil coolers. The engine cowling is of the NACA type C fitted with eight adjustable cowl flaps extending around the upper half of the cowling. A small fixed air gap between the engine cowling and the fuselage body extends around the lower half of the cowling to the auxiliary air-supply scoop. The opening of the auxiliary air-supply scoop, which supplies air to the carburetor, intercooler, oil coolers, and exhaust cooling shrouds, is located within the engine cowling at the bottom of the engine. The intercooler is mounted at the rear of the airplane slightly forward of

the turbosupercharger and is provided with two separate cooling-air outlets and flaps, one on each side of the fuselage. The oil coolers are mounted in series with respect to the oil flow, one on each corner of the fuselage at the rear of the engine.

Engine cooling-air pressure measurements. - Although the tests included an extensive cooling-air pressure survey in which a large number of pressure tubes and locations were used, only those tube combinations specified by recent NACA procedures as giving the best indication of the average cooling-air pressures ahead of and behind the engine are of present interest. The tubes used for the average pressure indications and their locations are shown in figure 3.

The total pressure of the cooling air was measured ahead of the engine with open-end tubes H1, H2, H3, and H4 located on each front-row cylinder at the positions indicated in figure 3. These tubes were installed halfway between the fin tips and the cylinder baffle at a point about one-eighth inch behind the tangent point of the baffle-entrance curl. The cooling-air static pressure behind the engine was measured on each rear-row cylinder with open-end tube P3 installed in the stagnation region behind the cylinder top baffle and tubes P1 and P4 installed in the curl of the intake-side baffle. Care was taken in the installation of these tubes to insure that they received little if any velocity head.

The pressure tubes were led to motor-driven pressure-selector valves which, in turn, were connected to NACA recording multiple manometers. All pressures could be recorded in 2 minutes.

Temperature measurements. - Cylinder-wall temperatures were measured with iron-constantan thermocouples located on the heads and the barrels of each of the 18 engine cylinders. The locations and designations of these cylinder-wall thermocouples are indicated in figure 4 and are as follows:

(1) At the rear spark plug with standard gasket-type thermocouple T12. (See fig. 5 for sketch of gasket details.)

(2) In the rear spark-plug boss with thermocouple T35 embedded to a depth of one-sixteenth inch. (See fig. 5 for details of installation.)

(3) In the rear middle of the head circumferential finning with thermocouple T19 peened about one-sixteenth inch into the cylinder-wall surface

4

(4) In the rear of the barrel two-thirds of the way up with thermocouple T6 peened about one-sixteenth inch into the aluminum-barrel muff

(5) At the rear of the cylinder base flange with thermocouple T14 spot-welded at the flange

The free-air temperature was obtained from the temperature reading of a resistance-bulb thermometer installed under and near the tip of the right wing. The correction for stagnation-heating effect was determined in a separate flight calibration for various airspeeds.

A survey of the temperatures in the cooling-air stream directly behind the engine was made during most of the flight tests. Eighteen iron-constantan thermocouples were used in this survey, two in front of each of the nine intake pipes at the same radial distances as the middle of the engine heads and barrels. The intake pipes provided partial shielding of the thermocouples from the exhaust-collector ring.

The temperature of the charge air was measured at the carburetor top deck with four parallel-connected iron-constantan thermocouples.

All temperatures were recorded by high-speed data recorders consisting of galvanometers, thermocouple selector switches, and film-drum recorders. It was possible to record 200 temperatures during each run in about 3 minutes. A calibration point was obtained for each galvanometer during each test run by taking galvanometer readings of a known standard voltage; the effect of changing galvanometer calibration was thus eliminated. A check on the accuracy of the temperature records was also provided during each run by recording on each galvanometer the temperature of hot mercury contained within a thermos bottle.

Charge-air-weight-flow measurements. - The charge-air weight flow was measured during flight by venturi meters installed in the two parallel lines between the intercooler and carburetor, as shown in figure 2, and calibrated within the charge-air ducting system prior to the flight tests. In addition, checks were obtained from the carburetor compensated metering pressure as measured during flight and its relation with charge-air flow as established in extensive carburetor air-box tests for the test range of carburetor pressures and temperatures. The checks obtained were within ±3 percent, the deviations being of a random nature.

Fuel-flow measurements. - A flow-bench calibration of the car-
buretor in which the fuel flow was related to the carburetor com-
pensated metering pressure furnished the most direct and simplest
method of measuring fuel flow in the flight tests. This fuel-flow
calibration was later verified in the air-box tests, which showed
the relation between compensated metering pressure and fuel flow
to be independent of the pressure and temperature conditions of the
charge air at the carburetor top deck and also of the fuel tempera-
ture, within the range encountered. In addition, fuel-flow checks
were obtained with both a vane-type and a rotameter-type fuel flow-
meter in several special flights covering the engine fuel-flow
operating range. Except for a few widely erratic points, the
checks were within ±3 percent.

Other measurements. - Free-stream impact pressure was measured
by a shrouded total-head tube installed on a streamline boom on
the right wing tip. A swiveling static tube, which was calibrated
in a special flight, was also carried by the boom about 1 chord
length ahead of the leading edge of the wing. Continuous records
of both the impact and static pressures were taken during each run
by NACA pressure recorders.

A torquemeter was incorporated for measuring engine torque.
The torque was indicated on a gage in the cockpit and was read by
the pilot.

Engine and turbine speeds were separately recorded by revolu-
tion counters operated in conjunction with a chronometric timer.

The engine exhaust pressure was measured by means of static
wall taps located on both sides of the exhaust collector ring
upstream of the waste gate.

Continuous records were taken on NACA pressure and control-
position recorders of manifold pressure; charge-air pressure at
the turbosupercharger outlet and at the carburetor top deck; throttle
setting; mixture-control setting; angle of attacks; and engine, oil
cooler, and intercooler flap openings.

TEST PROCEDURE

The flight tests were conducted, for the most part, at alti-
tudes (based on pressure) of 5000, 25,000, 30,000, and 35,000 feet;
a few flights were also made at intermediate altitudes. The three
main controllable variables during each test run at a given altitude
were engine power, engine speed, and engine cooling-air pressure

drop; in general, during each constant-altitude flight one of these three variables was independently varied while the other two were maintained constant.

The engine power was controlled with the carburetor throttle at constant engine speed and, at the high altitudes, also with the exhaust waste gate through regulation of the turbosupercharger speed. The mixture control was set in the automatic-rich position and the fuel-air ratio was allowed to vary according to the carburetor characteristics. The engine speed was controlled with the propeller governor and the cooling-air pressure drop was controlled by means of the cowl-flap deflection and through change in the airplane drag characteristics (and thus the airplane velocity and available ram pressure) obtained by raising and lowering the landing gear.

A summary of the flight test conditions is presented in table I. During each test run, in which the specified test conditions were held constant and the cylinder-wall temperatures had been stabilized, a record was obtained of the cooling-air pressures and temperatures ahead of and behind the engine, the cylinder-wall temperatures, and the airplane and engine operating conditions.

REDUCTION OF COOLING DATA

Correlation equations. - The basic equation developed in reference 1 for correlating the wall temperatures of air-cooled engines with the engine operating conditions and the cooling-air temperature and weight flow is

$$\frac{T_h - T_a}{T_g - T_h} \bigg/ W_c{}^n = \frac{K_1}{W_a{}^r} \tag{1}$$

All symbols are defined in appendix A.

It has been the practice in low-altitude cooling-correlation work to assume that the weight flow of cooling air W_a is a function of the more readily measured quantity $\sigma_{en}\Delta p$ and to make this substitution in equation (1). The assumption that W_a is a unique function of $\sigma_{en}\Delta p$ has, however, been shown by various theoretical analyses (references 4, 5, and 7) and some test data (reference 6) to be inaccurate for large altitude changes.

It is shown in appendix B, which presents a theoretical treatment of the relation between cooling-air weight flow and pressure

drop, that W_a is, more correctly, a function of σ_{ex}/σ_{en} in addition to $\sigma_{en}\Delta p$. On the basis of the results of appendix B, equation (1) is written

$$\frac{T_h - T_a}{T_g - T_h}\bigg/ W_c^{\,n} = \frac{K_2}{(\sigma_{en}\Delta p)^m}\; \phi\left(\frac{\sigma_{ex}}{\sigma_{en}}\right) \tag{2}$$

where $\phi\left(\sigma_{ex}/\sigma_{en}\right)$ denotes a function of σ_{ex}/σ_{en}.

At low altitudes, the variation of σ_{ex}/σ_{en} over the normal engine operating range is sufficiently small that its function may be considered as a constant, with negligible sacrifice in accuracy. For substantially constant σ_{ex}/σ_{en} equation (2) becomes the familiar correlation equation

$$\frac{T_h - T_a}{T_g - T_h}\bigg/ W_c^{\,n} = \frac{K_3}{(\sigma_{en}\Delta p)^m} \tag{2a}$$

When a large altitude range is considered, in which case large variations in σ_{ex}/σ_{en} are encountered, it is necessary to include the variations of the function $\phi(\sigma_{ex}/\sigma_{en})$ in equation (2). In appendix B, $\phi\left(\sigma_{ex}/\sigma_{en}\right)$ is theoretically derived. If it is assumed that

$$\phi\left(\frac{\sigma_{ex}}{\sigma_{en}}\right) = K_4\left(\frac{\sigma_{ex}}{\sigma_{en}}\right)^{-b}$$

equation (2) reduces to

$$\frac{T_h - T_a}{T_g - T_h}\bigg/ W_c^{\,n} = \frac{K}{(\sigma_{en}\Delta p)^m\left(\dfrac{\sigma_{ex}}{\sigma_{en}}\right)^b} \tag{3}$$

the constants n, m, b, and K will be evaluated from the test data.

In order for exit density (as suggested in references 5 and 6, and as theoretically shown in reference 7) to be a satisfactory basis of correlation it is necessary that $b = m$ in equation (3), in which case equation (3) reduces to

$$\frac{T_h - T_a}{T_g - T_h}\bigg/ W_c{}^n = \frac{K}{(\sigma_{ex}\Delta p)^m} \tag{4}$$

The accuracy of the foregoing simplification will be empirically checked with the flight-test data. Equations similar to equations (1) to (4) may also be written for the engine barrels.

Some investigators (see, for example, reference 8) believe that, in order to obtain accurate correlation, the local cooling-air temperature in the vicinity of the spot on the cylinder wall under investigation (at the location where T_h is measured) should be used instead of the entrance cooling-air temperature. In appendix C it is shown that the cooling-correlation equation containing the local cooling-air temperature can be transposed to the equation containing entrance cooling-air temperature; hence either can be used. The inlet cooling-air temperature was used in the correlation presented in this report because the added complication of determining the local cooling-air temperature did not appear warranted.

Mean effective gas temperature T_g. - The mean effective gas temperature T_g is, for a given engine, considered a function of fuel-air ratio, inlet-manifold temperature, exhaust pressure, and spark timing.

On the basis of previous correlation work, a $T_{g_{80}}$ value of 1150° F for the heads and 600° F for the barrels is chosen for the reference conditions of $F/A = 0.08$, $T_m = 80^\circ$ F, and $p_e = 30$ inches of mercury absolute, and for the normal spark setting.

The variation of $T_{g_{80}}$ with fuel-air ratio for the sea-level exhaust-pressure condition is taken as that determined in previous cooling tests on an R-2800-21 single-cylinder engine (reference 9). This $T_{g_{80}}$ variation, which was also found to check well with the results obtained on other types and models of air-cooled engines, is plotted for the heads and barrels in figure 6. The variation of $T_{g_{80}}$ with exhaust pressure for the range covered in the present tests is included in figure 6 and represents the results of extensive exhaust-pressure tests conducted at Cleveland on an R-2800-5 engine. Inasmuch as the engine normal spark timing was used throughout the tests, the effect of this variable is not required for analysis of the cooling test data.

9

The correction applied to $T_{g_{80}}$ to obtain T_g for values of T_m other than 80° F is given as $\Delta T_g = 0.8\,(T_m - 80)$ for engine heads and $\Delta T_g = 0.5\,(T_m - 80)$ for engine barrels. The dry inlet-manifold temperature T_m is calculated from the carburetor inlet-air temperature and the theoretical blower temperature rise, assuming no fuel vaporization. This relation is given as

$$T_m = T_c + \frac{U^2}{gJc_p} \tag{5}$$

For the engine used in the present investigation, equation (5) reduces to

$$T_m = T_c + 22.1\left(\frac{N}{1000}\right)^2 \tag{6}$$

Cylinder temperatures. - The value of cylinder-head temperature T_h used in the primary correlation is taken as the average for the 18 cylinders of the temperature indications of the thermocouples peened into the rear middle of the heads (T19 in fig. 4); the barrel temperature T_b is taken as the average of the temperature indications of the thermocouples peened into the rear of the barrels (T6 in fig. 4). Final correlation curves based on the rear-spark-plug-gasket and boss embedded-thermocouple readings (T12 and T35 in fig. 4) are also presented to permit cooling comparisons with the results of other investigations.

Cooling-air temperatures. - The entrance cooling-air temperature T_a is taken as the stagnation air temperature ahead of the engine as calculated from the free-air temperature and the airplane velocity measurements.

The exit cooling-air temperature, which is required for calculation of the exit density, was obtained for about 90 percent of the tests from the average of the temperature indications of the thermocouples located in the cooling-air stream behind the engine, the values for the engine-head and engine-barrel cooling air being separately averaged. These data were correlated by means of a relation developed in appendix D, which results in a single curve involving the cooling-air pressure drop and the ratio of the temperature rise of the cooling air ΔT to the temperature difference between the cylinder head and the entrance cooling air $T_h - T_a$. In the correlation of the cooling-test data, the exit cooling-air temperatures for all the tests are calculated from this curve.

Cooling-air pressure drop and density. - The average cooling-
air pressure drops across the engine heads and barrels are separately
determined as the difference between the average total pressure ahead
of and the average static pressure behind the engine heads or bar-
rels.

The average for the front-row cylinders of the readings of the
tubes designated H1, H2, and H3 (fig. 3) is taken as the average
pressure in front of the engine heads; the average of the readings
of the tubes H4 is taken as the average pressure in front of the
engine barrels.

The average static pressure behind the engine heads is obtained
from the average for the rear-row cylinders of the readings of
tubes P1 and P2; tubes P4 are used for obtaining the average static
pressure behind the engine barrels.

The entrance density of the cooling air is calculated from the
stagnation-air temperature and the total-pressure values ahead of
the engine; conversion into entrance density ratio σ_{en} is made
simply by dividing by the standard sea-level density value
(0.0765 lb/cu ft). The exit density of the cooling air is calcu-
lated from the exit-air-temperature and static-pressure values
behind the engine and is converted into exit density ratio σ_{ex}
by dividing by standard sea-level density.

Although the exit density is readily calculated from the
measurements of temperature and pressure made in the flight tests,
its evaluation for use in predicting cooling performance from an
established correlation is not direct inasmuch as it involves a
knowledge of the temperature rise and pressure drop of the cooling
air across the engine. A method of calculating the exit density
for use in cooling predictions is given in appendix E.

Constants m, n, and K_3. - The exponents m and n of $\sigma_{en}\Delta p$
and W_c, respectively, and the constant K_3 are determined from
the cooling data obtained at a constant σ_{ex}/σ_{en} (for all practical
purposes, at a constant altitude) by means of the familiar corre-
lation procedure expressed in equation (2a).

The function $\phi(\sigma_{ex}/\sigma_{en})$. - In order to check the validity of
the theoretically derived equations (3) and (4), the function
$\phi(\sigma_{ex}/\sigma_{en})$, which represents the effect of cooling-air compressi-
bility in the generalized correlation equation (equation (2)), is

experimentally determined by plotting $\dfrac{T_h - T_a}{T_g - T_h} \dfrac{(\sigma_{en}\Delta p)^m}{W_c^n}$ against

σ_{ex}/σ_{en} from the data obtained at the different altitudes. In order to minimize the extraneous effects resulting from differences in engine operating conditions that may not correlate accurately and may therefore mask the less sensitive effects of the cooling-air density change, data are selected, in the construction of this plot, for a narrow range of engine operating conditions (1200 and 1500 bhp; engine speed, 2550 rpm; fuel-air ratio, 0.12). In addition, in order to increase the over-all accuracy of the plotted parameters through reduction of the random percentage errors associated with the tests, the values of the parameters for the individual runs of each variable cooling-air pressure flight (five to six runs per flight) are averaged to give one plotted point per flight.

RESULTS AND DISCUSSION

Determination of constants m, n, and K_3. - The determination of the exponent m on $\sigma_{en}\Delta p$ (equation (2)) is shown in figure 7 where plots of $\dfrac{T_h - T_a}{T_g - T_h}$ and $\dfrac{T_b - T_a}{T_g - T_b}$ against $\sigma_{en}\Delta p$ are made from the data obtained at an approximately constant σ_{ex}/σ_{en} value of 0.83 (constant altitude of 5000 ft) in flights that were each conducted at substantially constant charge-air weight flow, fuel-air ratio, and engine speed with variable cooling-air pressure drop. Lines with the best-fitting constant slope are drawn through the plotted values for each of the flights. The common slope, which is the negative value of m in equation (2), is -0.35 for the engine heads and -0.43 for the engine barrels.

A cross plot from figure 7 of the values of $\dfrac{T_h - T_a}{T_g - T_h}$ and $\dfrac{T_b - T_a}{T_g - T_b}$ against charge-air weight flow W_c for a constant $\sigma_{en}\Delta p$ value of 12 inches of water for the heads and 9 inches of water for the barrels is presented in figure 8. Included in this figure are the cooling results obtained in a single flight conducted for variable charge-air weight flow at an approximately constant σ_{ex}/σ_{en} value of 0.83 and $\sigma_{en}\Delta p$ values of 12 and 9 inches of water for the heads and barrels, respectively. The plotted values for the variable charge-air-flow flight fall in with the points taken from the cross plot of figure 7. These points determine a slope of 0.60 for the heads and 0.43 for the barrels, which are the respective values of n (equation (2)) for the engine heads and barrels.

The values of $\dfrac{T_h - T_a}{T_g - T_h}\bigg/W_c^{0.60}$ and $\dfrac{T_b - T_a}{T_g - T_b}\bigg/W_c^{0.43}$, as cal-
culated from the data obtained in all the flights conducted at
σ_{ex}/σ_{en} of approximately 0.83 (altitude, 5000 ft), are plotted in
figure 9 against the corresponding $\sigma_{en}\Delta p$ values. A line with
the previously determined slope $-m$ (-0.35 for the heads and -0.43
for the barrels) is drawn to best represent the plotted values.
The correlation equation, which represents the correlation line
drawn in figure 9 for σ_{ex}/σ_{en} of 0.83, is expressed as

$$\frac{T_h - T_a}{T_g - T_h}\bigg/W_c^{0.60} = \frac{0.42}{(\sigma_{en}\Delta p)^{0.35}} \tag{7}$$

For the engine barrels

$$\frac{T_b - T_a}{T_g - T_b}\bigg/W_c^{0.43} = \frac{0.85}{(\sigma_{en}\Delta p)^{0.43}} \tag{8}$$

It is noted that the constant of 0.42 in equation (7) and 0.85
in equation (8) are equal to K_2 $(\sigma_{ex}/\sigma_{en})$ in the general corre-
lation expression (equation (2)) and to K_3 in equation (2a).

Determination of function $\phi(\sigma_{ex}/\sigma_{en})$. - In accordance with
equation (2) the values of $\dfrac{T_h - T_a}{T_g - T_h}\dfrac{(\sigma_{en}\Delta p)^{0.35}}{W_c^{0.60}}$ averaged for each
flight at constant engine conditions but variable cooling-air
pressure drop are plotted in figure 10 against the corresponding
σ_{ex}/σ_{en} values. The plotted points define a variation of increasing
$\phi(\sigma_{ex}/\sigma_{en})$ with decreasing σ_{ex}/σ_{en} thus indicating the detri-
mental effect of cooling-air compressibility on engine cooling.
This effect is the well known altitude effect, which, for constant
$\dfrac{T_h - T_a}{T_g - T_h}\bigg/W_c^{n}$ is reflected as an increase $\sigma_{en}\Delta p$ requirement with
increased altitude. Curves describing the theoretical variations
of $\phi(\sigma_{ex}/\sigma_{en})$ with σ_{ex}/σ_{en}, as determined in appendix B, are
included in figure 10 for comparison. Agreement with the experi-
mental results is indicated.

It is evident that the exponent b in equation (3) is equal
numerically to the slope of a straight line through the points in
figure 10. A line having a slope of -0.35 (the negative value of

the exponent m of $\sigma_{en}\Delta p$ in equation (7)) is drawn through the point representing the data at an altitude of 5000 feet. This line gives a good representation of the test data and also of the theoretical curves and is arbitrarily chosen as it permits simplification of equation (3) to equation (4).

The correlation equation for the cylinder heads obtained from figure 10 is

$$\frac{T_h - T_a}{T_g - T_h} \bigg/ W_c^{0.60} = \frac{0.39}{(\sigma_{en}\Delta p)^{0.35} \left(\dfrac{\sigma_{ex}}{\sigma_{en}}\right)^{0.35}} = \frac{0.39}{(\sigma_{ex}\Delta p)^{0.35}} \qquad (9)$$

It is noted that the constant of 0.39 in equation (9) is the test value of K in equation (4). When σ_{ex}/σ_{en} is set equal to 0.83, (value for tests at an altitude of 5000 ft), equation (9) reduces to equation (7).

Attempts to determine the function $\phi(\sigma_{ex}/\sigma_{en})$ for the cylinder barrels by the foregoing method were unsuccessful because of the large scatter of data, which masked the effect of the function $\phi(\sigma_{ex}/\sigma_{en})$ on the barrel cooling. In the correlation of the barrel data presented in the subsequent section it will be assumed, however, that the function $\phi(\sigma_{ex}/\sigma_{en})$ for the barrels is similar to that for the heads and that the exponent b is equal to the value of m for the barrels (0.43).

Correlation of all data on basis of $\sigma_{ex}\Delta p$. - The values of $\dfrac{T_h - T_a}{T_g - T_h} \bigg/ W_c^{0.60}$ and $\dfrac{T_b - T_a}{T_g - T_b} \bigg/ W_c^{0.43}$ calculated from the data obtained in all the flight tests covering a range of altitudes from 5000 to 35,000 feet (equivalent to a range of σ_{ex}/σ_{en} from 0.83 to 0.62) are plotted in figure 11 against the corresponding $\sigma_{ex}\Delta p$ values. The correlation line given by equation (9) for the engine heads is indicated in figure 11. It is readily evident that this single correlation line well represents both the low-altitude and the high-altitude cooling data. The best line with the previously determined slope of -0.43 is drawn through the plotted values for the barrel. It is evident that for the data on the barrel the agreement between the plotted values and the line is only fair at the high-altitude conditions but that no definite conclusions can be drawn because of the large data scatter. The equation that describes this line is

14

$$\frac{T_b - T_a}{T_g - T_b} \bigg/ W_c^{0.43} = \frac{0.77}{(\sigma_{ex}\Delta p)^{0.43}} \tag{10}$$

Correlation of all data on basis of $\sigma_{en}\Delta p$. - The variable-altitude cooling data is plotted against $\sigma_{en}\Delta p$ in figure 12 wherein comparison is made with the correlation line given for σ_{ex}/σ_{en} equal to 0.83 (5000-ft altitude) by equations (7) and (8) for the engine heads and barrels, respectively. It is seen that because of the test variation of σ_{ex}/σ_{en}, which is not accounted for by the correlation line, the test points obtained at the high altitudes, although quite scattered, tend to fall slightly above the correlation line and show a definite trend of increasing deviation with increase in altitude. This general grouping of the high-altitude data points above the 5000-foot correlation line again indicates a greater $\sigma_{en}\Delta p$ requirement at the higher altitudes. Even for as high an altitude as 35,000 feet, however, the deviations are only of the same order as the spread in the test points.

An examination of the plotted points in figure 12 indicates that a single line with a slightly higher slope than the correlation line for constant σ_{ex}/σ_{en} can be drawn to fit satisfactorily all the data. This apparent data correlation can be explained with reference to figure 13, which presents, for the same data as in figure 12, a plot of σ_{ex}/σ_{en} against $\sigma_{en}\Delta p$ on logarithmic coordinate paper. It is noted that, although the relation between σ_{ex}/σ_{en} and $\sigma_{en}\Delta p$ is actually different for the different altitudes, the bulk of the data for the entire altitude test range can be roughly represented by a single relation expressed as $\sigma_{ex}/\sigma_{en} = K_5 (\sigma_{en}\Delta p)^s$. The use of a single relation is made possible in this case only because of the operational limitations of the engine-airplane combination that causes a shift in operating range of $\sigma_{en}\Delta p$ with altitude; for example, at an altitude of 5000 feet (σ_{ex}/σ_{en} = approximately 0.83), a range of $\sigma_{en}\Delta p$ of approximately 4 to 20 inches of water was covered in the tests, whereas at an altitude of 30,000 feet (σ_{ex}/σ_{on} = approximately 0.75), the $\sigma_{en}\Delta p$ range is approximately 1.5 to 5.5 inches of water. Substitution of $K_5 (\sigma_{en}\Delta p)^s$ for σ_{ex}/σ_{on} and the value of m for b in equation (3) reduces the right-hand term of this equation to $K_6/(\sigma_{en}\Delta p)^{m(1+s)}$, which gives $m(1+s)$ as the slope of the line best correlating the plotted points in figure 12. Inasmuch as the establishment of this correlation is dependent on the variation obtained in the tests of σ_{ex}/σ_{on} with $\sigma_{en}\Delta p$, it is applicable,

for use in predictions, only when the operating conditions satisfy the test relation between σ_{ex}/σ_{en} and $\sigma_{en}\Delta p$. This correlation is therefore of no reliable aid in altitude and pressure-drop extrapolations.

Correlation of average rear-spark-plug-boss and gasket temperatures. - Inasmuch as the cooling of aircraft engines is frequently evaluated on the basis of the rear-spark-plug-boss and gasket temperatures, the correlation results based on these temperature readings (T35 and T12 in fig. 4) are presented in figures 14 and 15 as plots of $\dfrac{T35 - T_a}{T_g - T35}\Big/ W_c^{0.60}$ and $\dfrac{T12 - T_a}{T_g - T12}\Big/ W_c^{0.60}$, respectively, against $\sigma_{ex}\Delta p$ and $\sigma_{en}\Delta p$. It is of interest to know, as an indication of the accuracy of the general test results, that the correlation line for the rear-spark-plug-boss temperature checks within an average accuracy of 10° F with that obtained in an NACA test-stand investigation of a similar multicylinder engine.

Altitude cooling predictions from sea-level correlation. - A comparison of the cooling obtained at altitude, as predicted by the cooling-correlation line based on $\sigma_{ex}\Delta p$ (equation (9)) with that indicated by the sea-level cooling-correlation (actually 5000-ft altitude) line based on $\sigma_{en}\Delta p$ (equation (7)) is shown in figure 16 as a plot of average head temperature T19 against altitude for constant engine conditions and two constant values of cooling-air pressure drop (10 and 20 in. of water). The difference between the curve based on $\sigma_{ex}\Delta p$ and that based on $\sigma_{en}\Delta p$ amounts to 9° F at 20,000 feet, 13° F at 30,000 feet, and 36° F at 50,000 feet, when the cooling-air pressure drop is 10 inches of water. For a cooling-air pressure drop of 20 inches of water, differences of 9°, 20°, and 60° F are obtained for 20,000, 30,000, and 50,000 feet, respectively.

The magnitude of the errors introduced when predicting high-altitude pressure-drop requirements from the low-altitude correlation line based on $\sigma_{en}\Delta p$ rather than $\sigma_{ex}\Delta p$ is illustrated in figure 17, which presents, for a given set of constant engine operating conditions, the cooling-air pressure-drop variation with altitude as calculated by both correlations for maintaining an average head temperature of 400° F. Errors in cooling-air pressure drop of 1, 2, and 14 inches of water are indicated for 20,000, 30,000, and 50,000 feet, respectively.

Figures 16 and 17 indicate that altitude predictions from a sea-level correlation based on $\sigma_{en}\Delta p$ are fairly accurate up to

20,000 feet but that the error increases so rapidly with further increase in altitude that the correlation based on $\sigma_{ex}\Delta p$ should be used at the higher altitudes.

CONCLUSIONS

The results of engine-cooling flight tests conducted on an 18-cylinder, twin-row, radial, air-cooled engine in a pursuit airplane for a range of altitudes from 5000 to 35,000 feet show that:

1. The effect of cooling-air compressibility on the cooling characteristics of air-cooled engines can be accounted for, to a good degree of accuracy, by the use in the NACA cooling correlation method of the cooling-air pressure drop based on the exit rather than the commonly used entrance density. The use of exit density is further rationalized theoretically.

2. A sea-level correlation on the basis of entrance density gives fairly accurate results up to an altitude of 20,000 feet. For higher altitudes, however, the use of exit density wherever possible is recommended inasmuch as the error resulting from the use of entrance density increases at a rapidly increasing rate with altitude.

3. For an illustrative set of constant engine operating conditions, the errors involved in predictions made from the low-altitude correlation based on entrance rather than exit density amount to:

(a) Average head temperatures of 9°, 13°, and 36° F for a constant cooling-air pressure drop of 10 inches of water at 20,000, 30,000, and 50,000 feet, respectively.

(b) Cooling-air pressure drops of 1, 2, and 14 inches of water for an average head temperature of 400° F at 20,000, 30,000, and 50,000 feet, respectively.

Aircraft Engine Research Laboratory,
    National Advisory Committee for Aeronautics,
        Cleveland, Ohio, May 9, 1946.

APPENDIX A

SYMBOLS

All symbols used in the text and the appendixes are defined here in alphabetical order for convenience of reference.

A outside-wall area of cylinder head, sq in.

c_p specific heat of air, 0.24 Btu/(lb)(°F)

f cylinder free-flow area ratio

F cylinder friction factor

F_1 cylinder friction factor at $\sigma_{en}\Delta p = 1$ in. of water

F/A fuel-air ratio of engine charge

g acceleration of gravity, 32.2 ft/sec^2

h heat-transfer coefficient from outside wall of cylinder head to cooling air, Btu/(sq in.)(°F)(sec)

J mechanical equivalent of heat, 778 ft-lb/Btu

N engine speed, rpm

p absolute pressure of cooling air, in. Hg

p_e engine absolute exhaust pressure, in. Hg

Δp cooling-air pressure drop across engine, in. water

Δp_f cooling-air pressure drop due to skin friction within cylinder interfin passages, in. water

Δp_m cooling-air pressure drop due to momentum change of cooling air across cylinder, in. water

T_a cooling-air temperature ahead of engine, °F

T_r cooling-air temperature at rear of engine, °F

T_b cylinder-barrel temperature, °F

T_c carburetor inlet-air temperature, °F

T_g mean effective gas temperature, °F

T_{g80} mean effective gas temperature corrected to a dry inlet-manifold temperature of 80° F

T_h cylinder-head temperature, °F

T_m dry inlet-manifold temperature, °F

ΔT cooling-air temperature rise across engine, °F

U tip speed of engine-stage blower, ft/sec

V cooling-air velocity within interfin passages, ft/sec

W_a cooling-air weight flow across engine, lb/sec

W_c engine charge-air consumption, lb/sec

ρ cooling-air density, lb/cu ft

σ density of cooling air relative to standard air density of 0.0765 lb/cu ft, $\rho/0.0765$

Subscripts:

en   at cylinder entrance

ex   at cylinder exit

av   average condition between entrance and exit

Correlation constants:

$k, k_1, k_2, k_3, k_4, k_5, K, K_1, K_2, K_3, K_4, K_5, K_6$

Correlation exponents:

$n, m, r, r', b, s, x, y, Z$

APPENDIX B

THEORETICAL DERIVATION OF EFFECT OF COOLING-AIR-DENSITY

CHANGE ON ENGINE COOLING

An expression will be derived for the cooling-correlation equation in which account is taken of the effect on the cooling-air pressure drop of the change in cooling-air density from the front to the rear of the cylinder. From this expression and the test data at low altitude (5000 ft) an equation is obtained by means of which the cooling of the engine at any altitude may be predicted.

In the derivation of the expression for the cooling-air pressure drop, simplifications are made that have been found to introduce a small inaccuracy.

Simplified pressure-drop equation. - With reference to figure 18, the pressure losses across an engine cylinder can be divided and expressed as follows: Entrance loss (station 0 to station 1)

$$\Delta p_{en} = \frac{1}{5.2g} \frac{\rho_{en}V_{en}^2}{2} (1 - f^2) \tag{11}$$

Skin-friction losses within the cylinder interfin passages, (station 1 to station 2)

$$\Delta p_f = \frac{F}{5.2g} \frac{\rho_{av}V_{av}^2}{2}$$

or, based on the entrance conditions and exit-entrance density ratio (σ_{av} is taken as the arithmetic average of σ_{en} and σ_{ex})

$$\Delta p_f = \frac{1}{5.2g} \frac{\rho_{en}V_{en}^2}{2} \left(\frac{2F}{1 + \frac{\sigma_{ex}}{\sigma_{en}}} \right) \tag{12}$$

Momentum loss (station 1 to station 2)

$$\Delta p_m = \frac{\rho_{en}V_{en}}{5.2g} (V_{ex} - V_{en})$$

or

$$\Delta p_m = \frac{1}{5.2g} \frac{\rho_{en}V_{en}^2}{2} \left[2\left(\frac{1}{\frac{\sigma_{ex}}{\sigma_{en}}} - 1 \right) \right] \qquad (13)$$

Exit-pressure recovery (station 2 to station 3)

$$\Delta p_{ex} = \frac{\rho_{ex}V_{ex}f}{5.2g} (fV_{ex} - V_{ex})$$

or

$$\Delta p_{ex} = \frac{1}{5.2g} \frac{\rho_{en}V_{en}^2}{2} \left(\frac{2(f^2 - f)}{\frac{\sigma_{ex}}{\sigma_{en}}} \right) \qquad (14)$$

The total pressure loss across an engine cylinder is given by the summation of the component losses as

$$\Delta p = \frac{1}{5.2g} \frac{\rho_{en}V_{en}^2}{2} \left[(1 - f^2) + \frac{2F}{1 + \frac{\sigma_{ex}}{\sigma_{en}}} + 2\left(\frac{1}{\frac{\sigma_{ex}}{\sigma_{en}}} - 1 \right) + \frac{2(f^2 - f)}{\frac{\sigma_{ex}}{\sigma_{en}}} \right] \qquad (15)$$

Comparison between the values of pressure drop computed from equation (15) and from the more rigorous methods of reference 5 indicated a maximum difference of 10 percent for extreme conditions with respect to present cylinder and operating conditions.

Cooling-correlation equation including compressibility effect. - The simplified pressure-drop equation when solved for W_a, which is proportional to $\rho_{en}V_{en}$, can be written as

$$W_a = \frac{k_1(\sigma_{en}\Delta p)^{1/2}}{\left[(1 - f^2) + \frac{2F}{1 + \frac{\sigma_{ex}}{\sigma_{en}}} + 2\left(\frac{1}{\frac{\sigma_{ex}}{\sigma_{en}}} - 1 \right) + \frac{2(f^2 - f)}{\frac{\sigma_{ex}}{\sigma_{en}}} \right]^{1/2}} \qquad (16)$$

Substitution in the basic cooling-correlation equation (equation (1)) results in

$$\frac{\dfrac{T_h - T_a}{T_g - T_h}}{W_c^{\ n}} = \frac{K_1\left[(1-f^2)+\dfrac{2F}{1+\dfrac{\sigma_{ex}}{\sigma_{en}}}+2\left(\dfrac{1}{\dfrac{\sigma_{ex}}{\sigma_{en}}}-1\right)+\dfrac{2(f^2-f)}{\dfrac{\sigma_{ex}}{\sigma_{en}}}\right]^{r/2}}{k(\sigma_{en}\Delta p)^{r/2}} \qquad (17)$$

Multiplying both sides of equation (17) by $(\sigma_{en}\Delta p)^m$ gives

$$\frac{T_h - T_a}{T_g - T_h}\frac{(\sigma_{en}\Delta p)^m}{W_c^{\ n}} = \frac{K_1\left[(1-f^2)+\dfrac{2F}{1+\dfrac{\sigma_{ex}}{\sigma_{en}}}+2\left(\dfrac{1}{\dfrac{\sigma_{ex}}{\sigma_{en}}}-1\right)+\dfrac{2(f^2-f)}{\dfrac{\sigma_{ex}}{\sigma_{en}}}\right]^{r/2}}{k(\sigma_{en}\Delta p)^{r/2\ -\ m}} \qquad (18)$$

The friction factor F is proportional to the 0.2 power of the cooling-air Reynolds number for turbulent flow through the cylinder interfin passages. Because of this small variation of F with Reynolds number, the following simplifications in the determination of an expression for F are permissible:

(a) The viscosity in the Reynolds number parameter is assumed constant.

(b) The mass flow in the Reynolds number parameter is taken as proportional to $(\sigma_{en}\Delta p)^{1/2}$.

With these simplifications F can be written:

$$F = F_1(\sigma_{en}\Delta p)^{0.1} \qquad (19)$$

where F_1 is the value of F at $\sigma_{en}\Delta p$ equal to 1 inch of water.

Combination of equations (18) and (19) gives

$$\frac{T_h - T_a}{T_g - T_h}\frac{(\sigma_{en}\Delta p)^m}{W_c^{\ n}} = \frac{K_1}{k}\left[\frac{(1-f^2)+\dfrac{2F_1(\sigma_{en}\Delta p)^{0.1}}{1+\dfrac{\sigma_{ex}}{\sigma_{en}}}+2\left(\dfrac{1}{\dfrac{\sigma_{ex}}{\sigma_{en}}}-1\right)+\dfrac{2(f^2-f)}{\dfrac{\sigma_{ex}}{\sigma_{en}}}}{(\sigma_{en}\Delta p)^{1\ -\ \frac{2m}{r}}}\right]^{r/2} \qquad (20)$$

The left-hand side of equation (20) when equated to a constant is recognized as the usual form of the NACA correlation relation (equation 2(a)); the right-hand side introduces the effect of change in σ_{ex}/σ_{en}. The constants K_1/k, F_1, f, m, and r in equation (20) will be evaluated from the known air-flow characteristics of the engine cylinder and from the low-altitude test data (5000 ft) at which condition the value of σ_{ex}/σ_{en} was found to be effectively constant at 0.83 for a wide range of operating conditions. When the values of these constants are inserted in equation (20) this equation may be used to predict the cooling at other values of σ_{ex}/σ_{en} corresponding to any altitude and operation.

Evaluation of constants of equation (20). -

(a) The friction factor F_1 is determined as 0.9 from air-flow and pressure-loss data obtained at sea level in single-cylinder tests on an R-2800-21 engine.

(b) The value of free-flow area ratio f is taken as 0.1 as estimated from measurements on an R-2800-21 engine. An accurate value of f is not required as the terms involving f are small compared with the other terms in the numerator of the right-hand side of equation (20).

(c) The values of K_1/k and r are determined from the cooling-test data obtained for σ_{ex}/σ_{en} equal to 0.83 (5000-ft altitude tests) in the following manner:

For σ_{ex}/σ_{en} equal to 0.83, equation (20) must reduce to equation (7). Thus,

$$\frac{K_1}{k}\left[\frac{(1-f^2)+\dfrac{2F_1(\sigma_{en}\Delta p)^{0.1}}{1+0.83}+2\left(\dfrac{1}{0.83}-1\right)+\dfrac{2(f^2-f)}{0.83}}{(\sigma_{en}\Delta p)^{1-\frac{2m}{r}}}\right]^{r/2}=0.42 \quad (21)$$

On substitution of the numerical values of F_1 and f, and rearrangement, equation (21) becomes

$$1.184+0.984\,(\sigma_{en}\Delta p)^{0.1}=\left(0.42\,\frac{k}{K_1}\right)^{2/r}(\sigma_{en}\Delta p)^{1-\frac{2m}{r}} \quad (22)$$

When the left-hand side of equation (22) is plotted against $\sigma_{en}\Delta p$ on logarithmic coordinate paper, the slope equals the exponent $1-\dfrac{2m}{r}$.

Figure 19 presents this plot and indicates a value for $1 - \frac{2m}{r}$ of -0.04. The value of r, as calculated from this equality and the experimental value of m (indicated by equation (7) as equal to 0.35), is found to be 0.67. The ordinate in figure 19 at $\sigma_{en}\Delta p$ equal to 1 inch of water gives the value of $\left(0.42 \frac{k}{K_1}\right)^{2/r}$ as 2.2 from which $\frac{K_1}{k}$ is calculated to be 0.32. When the foregoing values are substituted for the constants and exponents, equation (20) becomes

$$\frac{T_h - T_a}{T_g - T_h}\frac{(\sigma_{en}\Delta p)^{0.35}}{W_c^{0.60}} = 0.32\left[\frac{0.99 + \dfrac{1.8(\sigma_{en}\Delta p)^{0.1}}{1 + \dfrac{\sigma_{ex}}{\sigma_{en}}} + 2\left(\dfrac{1}{\dfrac{\sigma_{ex}}{\sigma_{en}}} - 1\right) + \dfrac{-0.18}{\dfrac{\sigma_{ex}}{\sigma_{en}}}}{(\sigma_{en}\Delta p)^{0.04}}\right]^{0.335} \tag{23}$$

The value of $n = 0.60$ is obtained from the test data at 5000-foot altitude. The quantity $\frac{T_h - T_a}{T_g - T_h}\frac{(\sigma_{en}\Delta p)^{0.35}}{W_c^{0.60}}$ is computed from equation (23), which was established from the theoretical analysis and the cooling test data at σ_{ex}/σ_{en} equal to 0.83, and is plotted as dashed lines in figure 10 against σ_{ex}/σ_{en} for two extreme values of $\sigma_{en}\Delta p$(0.5 and 20 in. of water). It is noted that $\sigma_{en}\Delta p$ introduces negligible spread in the curves, which indicates that $\sigma_{en}\Delta p$ is of small significance in the right-hand side of equation (23) or its generalized form (equation (20)), and hence, that equation (23) can be approximated by equation (2).

APPENDIX C

JUSTIFICATION FOR USE OF INLET COOLING-AIR

TEMPERATURE IN CORRELATION EQUATIONS

The following derivation is presented to show the validity of the use in the correlation equations (for example, equation (1)) of the inlet cooling-air temperature instead of the local cooling-air temperature in the vicinity of the location at which the cylinder temperature is measured.

If the cylinder temperature at the rear of the head is under investigation then, on the basis of local cooling-air temperature, the correlation equation (1) would be written

$$\frac{T_h - T_r}{T_g - T_h} \bigg/ W_c{}^n = \frac{K_5}{W_a{}^{r'}} \qquad (24)$$

where the exponent r' differs numerically from the exponent r in equation (1).

From equations (28) and (29) developed in appendix D

$$T_r - T_a = \Delta T = \frac{k_2 \, A \, W_a{}^{(x-1)} \, (T_h - T_a)}{c_p} \qquad (25)$$

When T_r is eliminated from equation (24) by means of equation (25), there results

$$\frac{T_h - T_a - \dfrac{k_2 \, A \, W_a{}^{(x-1)}(T_h - T_a)}{c_p}}{(T_g - T_h) \, W_c{}^n} = \frac{K_5}{W_a{}^{r'}} \qquad (26)$$

Rearrangement of terms gives

$$\frac{T_h - T_a}{T_g - T_h} \bigg/ W_c{}^n = \frac{K_5}{W_a{}^{r'} \left[1 - \dfrac{k_2 \, A \, W_a{}^{(x-1)}}{c_p} \right]} \qquad (27)$$

It is noted that, for a given engine installation, the right-hand side of equation (27) is a function only of W_a and can be approximated within the limits of the variation of W_a of interest in engine cooling by $K_1/W_a{}^r$. Equation (27) then becomes

$$\frac{T_h - T_a}{T_g - T_h} \bigg/ W_c{}^n = \frac{K_1}{W_a{}^r} \qquad (28)$$

which is the same as equation (1) and similar in form to equation (24). It is thus evident that use of the inlet cooling-air temperature instead of the local cooling-air temperature merely results in a change of the constant and cooling-air exponent in the correlation equation.

If the assumption is made that the temperature rise of the cooling air to any given location around the cylinder as a percentage of the total temperature rise is constant for all operating conditions, then the same transformation from local-air temperature to inlet-air temperature as shown by equations (24) to (28) can be made for any local cylinder temperature.

APPENDIX D

ENGINE COOLING-AIR TEMPERATURE-RISE EQUATION

For convenience in cooling predictions, the engine cooling-air temperature rise is related to the other known cooling variables by equating the heat absorbed by the cooling air to the heat transferred from the cylinder walls to the cooling air. Thus,

$$W_a \, c_p \, \Delta T = h \, A \, (T_h - T_a) \tag{28}$$

Because

$$h = k_2 \, (W_a)^x \tag{29}$$

and

$$W_a = k_3 \, (\sigma_{ex} \Delta p)^y \tag{30}$$

solution for $\dfrac{\Delta T}{T_h - T_a}$ can be made in terms of $\sigma_{ex} \Delta p$,

$$\frac{\Delta T}{T_h - T_a} = k_4 \, (\sigma_{ex} \Delta p)^{y(x-1)} \tag{31}$$

The value of the exponent $y(x-1)$ is found from the test data to be 0.16 for the cylinder heads and 0.095 for the barrels. Because of the low values of this exponent, satisfactory correlation of $\dfrac{\Delta T}{T_h - T_a}$ with $\sigma_{en} \Delta p$ should also be obtainable; the use of $\sigma_{en} \Delta p$ rather than $\sigma_{ex} \Delta p$ is preferred in the $\dfrac{\Delta T}{T_h - T_a}$ relation because the results can then, in some applications, be more directly used with the correlation equation at little sacrifice in accuracy. Thus, for all practical purposes

$$\frac{\Delta T}{T_h - T_a} = k_5 (\sigma_{en} \Delta p)^Z \tag{32}$$

Plots of $\dfrac{\Delta T}{T_h - T_a}$ and $\dfrac{\Delta T}{T_b - T_a}$ against $\sigma_{en} \Delta p$ made from the cooling-test measurements are presented in figure 20 for the engine heads and barrels. The use of figure 20 for making altitude engine-cooling predictions is illustrated in appendix E.

APPENDIX E

HIGH-ALTITUDE ENGINE-COOLING PREDICTION

The use of $\sigma_{ex}\Delta p$ in the cooling-correlation equation, as required for accurately predicting cooling at altitude, introduces the troublesome problem of evaluating σ_{ex}. This problem is complicated by the fact that σ_{ex} is not directly obtainable from the atmospheric pressure and temperature values (including the corrections due to ram) as is the case with σ_{en} but further involves the engine heat rejection and cooling-air pressure drop. For this reason, simultaneous solution for σ_{en} and of the correlation equation is required; as direct solution is difficult, recourse is had to solution by the method of successive approximations.

The correlation relations that must be established in the low-altitude or sea-level engine-cooling tests for subsequent use in the determination of the cooling obtained at the high altitudes are, for the purpose of review, tabulated as follows:

1. The correlation equation (equation (4)) graphically represented for the subject tests by the correlation line of figure 11

2. The $T_{g_{80}}$ relation described by the curves of figure 6

3. The cooling-air temperature-rise equation (equation (32)) graphically represented in figure 20

The quantity σ_{ex}/σ_{on} is given by the general gas law

$$\sigma_{ex}/\sigma_{en} = \frac{p_{ex}}{p_{en}} \times \frac{T_a + 460}{T_r + 460} = \frac{1 - \dfrac{\Delta p}{p_{en}}}{1 - \dfrac{\Delta T}{T_a + 460}} \tag{33}$$

The quantity σ_{en} is calculated from the entrance cooling-air pressure and temperature. The quantity σ_{ex} can be computed from σ_{en} by means of equation (33).

For the purpose of illustrating the method of obtaining simultaneous solution of the foregoing pertinent relations to determine the cooling obtained at altitude, two typical problems are herein assumed and solved in step-by-step fashion.

Calculation of cooling-air pressure-drop requirements at altitude, case 1. -

The following operating conditions are assumed:

1. Engine charge-air consumption, lb/sec 3.5
2. Fuel-air ratio of charge 0.100
3. Dry inlet-manifold temperature, °F 250
4. Engine exhaust pressure, in. Hg absolute 30
5. Altitude of operation, ft 35,000

for which, including ram corrections,

$$T_a = 6° \text{ F}$$

$$p_{en} = 8.46 \text{ inches of mercury absolute}$$

It is required to find the cooling-air pressure drop Δp for satisfying the cooling requirement for an average rear-middle head temperature (T19 in fig. 4) of 400° F.

6. From figure 6 for items 2 and 4

$$T_{g_{80}} = 1000° \text{ F}$$

7. Correction of $T_{g_{80}}$ to a dry inlet-manifold temperature of 250° F gives

$$T_g = 1000 + 0.8 (250 - 80) = 1136° \text{ F}$$

8. From items 5 and 7 for $T_h = 400°$ F

$$\frac{T_h - T_a}{T_g - T_h} = \frac{400 - 6}{1136 - 400} = 0.535$$

9. From items 1 and 8

$$\frac{T_h - T_a}{T_g - T_h} \Big/ W_c^{0.60} = \frac{0.535}{3.50^{0.60}} = 0.252$$

10. From item 9 and equation (9) (or fig. 11)

$$\sigma_{ex} \Delta p = 3.5 \text{ inches of water}$$

Solution for σ_{ex} is now required and involves the method of successive approximation.

As the first approximation, assume

$$\sigma_{en} = \sigma_{ex}$$

11. Solution for σ_{en} from item 5 and the standard sea-level air conditions of a pressure of 29.92 inches of mercury absolute and a temperature of 519° R gives

$$\sigma_{en} = \frac{8.46}{29.92} \times \frac{519}{466} = 0.315$$

12. From items 10 and 11, the first approximation value of Δp is

$$\Delta p = \frac{3.5}{0.315} = 11.1 \text{ inches of water}$$

13. For $\sigma_{en}\Delta p = \sigma_{ex}\Delta p = 3.5$ inches of water (assumption in first approximation solution), figure 20 gives

$$\frac{\Delta T}{T_h - T_a} = 0.386$$

14. Thus from item 5 $(T_a = 6^{\circ}$ F) for $T_h = 400^{\circ}$ F

$$\Delta T = 0.386 \times 394 = 152^{\circ} \text{ F}$$

15. From equation (33) and items 5, 12, and 14

$$\frac{\sigma_{ex}}{\sigma_{en}} = \frac{1 - \dfrac{11.1}{13.6 \times 8.46}}{1 + \dfrac{152}{466}} = \frac{0.904}{1.326} = 0.682$$

which is the second approximation value of σ_{ex}/σ_{en}.

16. As the second approximation for Δp, from items 10, 11, and 15

$$\Delta p = \frac{3.5}{0.315 \times 0.682} = 16.3 \text{ inches of water}$$

17. From items 11 and 16

$$\sigma_{en}\Delta p = 0.315 \times 16.3 = 5.14 \text{ inches of water}$$

18. From figure 20 for item 17

$$\frac{\Delta T}{T_h - T_a} = 0.36$$

19. Thus from item 5 for $T_h = 400^\circ$ F

$$\Delta T = 0.36 \times 394 = 142^\circ \text{ F}$$

20. From equation (33) and items 5, 16, and 19

$$\frac{\sigma_{ex}}{\sigma_{en}} = \frac{1 - \dfrac{16.3}{13.6 \times 8.46}}{1 + \dfrac{142}{466}} = \frac{0.858}{1.305} = 0.658$$

which is the third approximation value of σ_{ex}/σ_{en}.

Thus, as the third approximation for Δp

$$\Delta p = \frac{3.5}{0.315 \times 0.658} = 16.9 \text{ inches of water}$$

Recalculation for σ_{ex}/σ_{en} gives a value of 0.654 as compared with 0.658 obtained in the third approximation. It is evident that the value of σ_{ex}/σ_{en} converges very rapidly and that a third approximation for σ_{ex}/σ_{en}, and thus for Δp, is sufficient.

The pressure-drop value of 16.9 inches of water obtained in the foregoing calculations compares with 13.6 inches of water, which would be given by the correlation based on $\sigma_{en}\Delta p$ (equation (7)).

Calculation of average head temperature obtained at altitude, case 2. - It is assumed that, for the conditions given in items 1 through 5, a cooling-air pressure drop of 10 inches of water is available for which it is desired to calculate the resulting head temperature.

21. From item 11 and for $\Delta p = 10$ inches of water

$$\sigma_{en}\Delta p = 3.15 \text{ inches of water}$$

22. From figure 20 and item 21

$$\frac{\Delta T}{T_h - T_a} = 0.39$$

23. As a first approximation, assume $T_h = 400^{\circ}$ F

Then, from items 5 $(T_a = 6^{\circ}$ F) and 22

$$\Delta T = 0.39 \times 394 = 154^{\circ} \text{ F}$$

24. From items 5, 23, and equation (33)

$$\frac{\sigma_{ex}}{\sigma_{en}} = \frac{1 - \dfrac{10}{13.6 \times 8.46}}{1 + \dfrac{154}{466}} = \frac{0.913}{1.33} = 0.686$$

25. From items 11 and 24 and for $\Delta p = 10$ inches of water

$$\sigma_{ex}\Delta p = 0.315 \times 0.686 \times 10 = 2.16 \text{ inches of water}$$

26. From equation (9) (or fig. 11) and item 25

$$\frac{T_h - T_a}{T_g - T_h} \bigg/ W_c^{0.60} = 0.298$$

27. From items 1, 5, 7, and 26

$$T_h = 442^{\circ} \text{ F}$$

28. As the second approximation, let

$$T_h = 442^{\circ} \text{ F}$$

Then from items 5 and 22

$$\Delta T = 0.39 \times 436 = 170^{\circ} \text{ F}$$

29. From items 5 and 28 and equation (33)

$$\frac{\sigma_{ex}}{\sigma_{en}} = \frac{1 - \dfrac{10}{13.6 \times 8.46}}{1 + \dfrac{170}{466}} = \frac{0.913}{1.365} = 0.668$$

30. From items 11 and 29 and for $\Delta p = 10$ inches of water

$$\sigma_{ex}\Delta p = 0.315 \times 0.668 \times 10 = 2.10 \text{ inches of water}$$

31. From equation (9) (or fig. 11) and item 30

$$\frac{T_h - T_a}{T_g - T_h}\bigg/ W_c^{0.60} = 0.301$$

32. From items 1, 5, 7, and 31

$$T_h = 446^{\circ} \text{ F}$$

which checks very closely with the second approximation value and is therefore the required value.

The derived T_h value of 446° F compares with 428° F, which would be obtained from the correlation based on $\sigma_{en}\Delta p$ (equation (7)).

REFERENCES

1. Pinkel, Benjamin: Heat-Transfer Processes in Air-Cooled Engine
   Cylinders. NACA Rep. No. 612, 1938.

2. Pinkel, Benjamin, and Rubert, Kennedy F.: Correlation of Wright
   Aeronautical Corporation Cooling Data on the R-3350-14 Inter-
   mediate Engine and Comparison with Data from the Langley
   16-Foot High-Speed Tunnel. NACA ACR No. E5A18, 1945.

3. Corson, Blake W., Jr., and McLellan, Charles H.: Cooling Char-
   acteristics of a Pratt & Whitney R-2800 Engine Installed in
   a NACA-Short-Nose High-Inlet Velocity Cowling. NACA ACR
   No. L4F06, 1944.

4. Becker, John V., and Baals, Donald D.: The Aerodynamic Effects
   of Heat and Compressibility in the Internal Flow Systems of
   Aircraft. NACA ACR, Sept. 1942.

5. Williams, David T.: High-Altitude Cooling. II - Air-Cooled
   Engines. NACA ARR No. L4I11a, 1944.

6. Pindzola, Michael: Cylinder Baffle Pressure Drop vs. Flow
   Characteristics of an Air-Cooled Engine Cylinder at Various
   Altitudes. PWA-505, Pratt & Whitney Aircraft, June 23, 1944.

7. Neustein, Joseph, and Schafer, Louis J., Jr.: Comparison of
   Several Methods of Predicting the Pressure Loss at Altitude
   across a Baffled Aircraft-Engine Cylinder. NACA TN No. 1067,
   1946.

8. Richards, William M. S., and Erdman, Frank H.: Prediction of
   Engine Cooling Requirements. SAE Jour. (Trans.), vol. 53,
   no. 7, July 1945, pp. 410-419.

9. Ellerbrock, Herman H., Jr., and Rollin, Vern G.: Correlation of
   Single-Cylinder Cooling Tests of a Pratt & Whitney R-2800-21
   Engine Cylinder with Wind-Tunnel Tests of a Pratt & Whitney
   R-2800-27 Engine. NACA ARR No. 3L14, 1943.

TABLE I - SUMMARY OF FLIGHT TEST CONDITIONS

Altitude (ft)	Engine power (bhp)	Pressure drop (in. water)	Engine speed (rpm)
5,000	800	Variable	2550
5,000	1000	---do---	2550
5,000	1300	---do---	2550
5,000	1500	---do---	2550
5,000	800	Constant	Variable
5,000	Variable	---do---	2550
5,000	1100	Variable	2550
5,000	Variable	Constant	2550
5,000	1000	---do---	Variable
5,000	Variable	Variable	2550
7,000	2000	---do---	2700
10,000	1500	---do---	2550
10,000	1000	---do---	Variable
15,000	1100	---do---	---do---
25,000	1000	---do---	2550
25,000	1100	---do---	2550
25,000	1000	---do---	2550
25,000	1500	---do---	2550
25,000	1800	---do---	2700
25,000	Variable	Constant	2550
25,000	1000	Variable	2550
25,000	Variable	---do---	2550
25,000	---do---	Constant	Variable
30,000	1300	Variable	2550
30,000	1500	---do---	2550
30,000	1100	---do---	2550
30,000	Variable	Constant	2600
35,000	1200	Variable	2550
35,000	1200	---do---	2550

National Advisory Committee
for Aeronautics
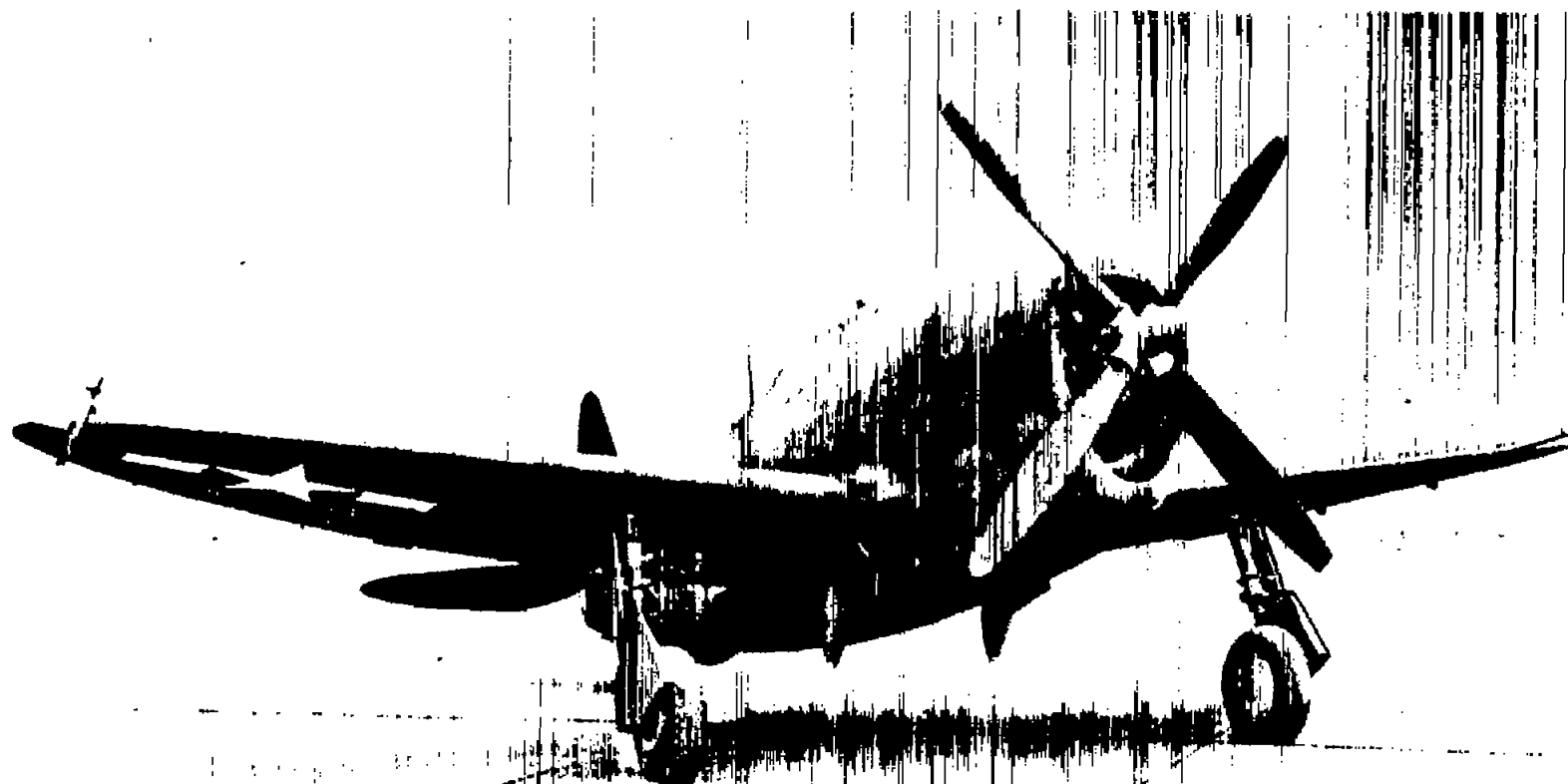
Fig. 1

AERL
3480

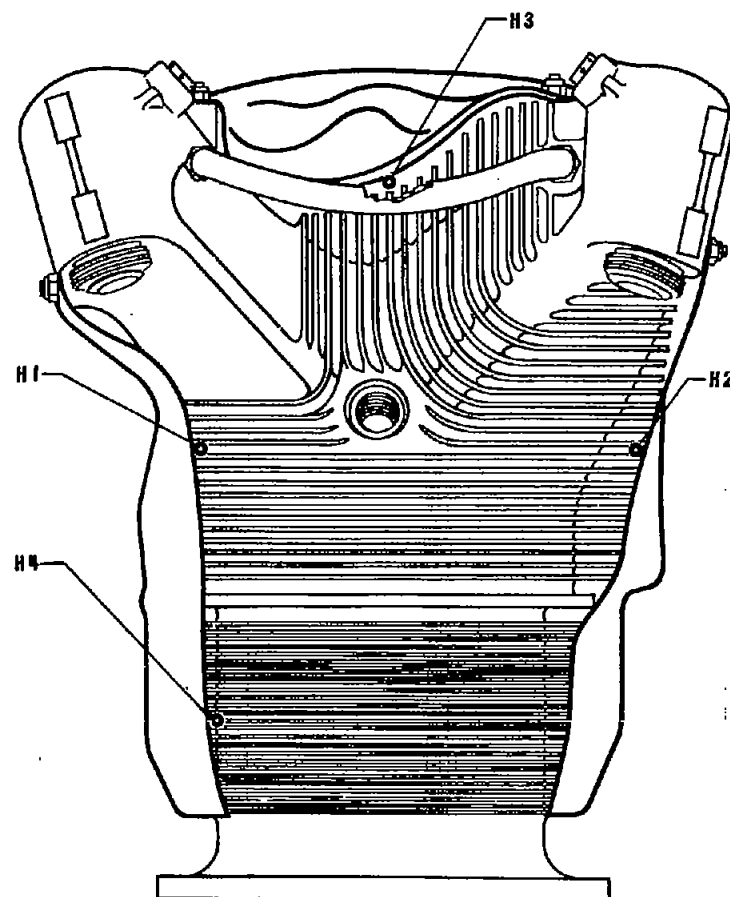Figure I. - Airplane used in the engine-cooling flight investigation.
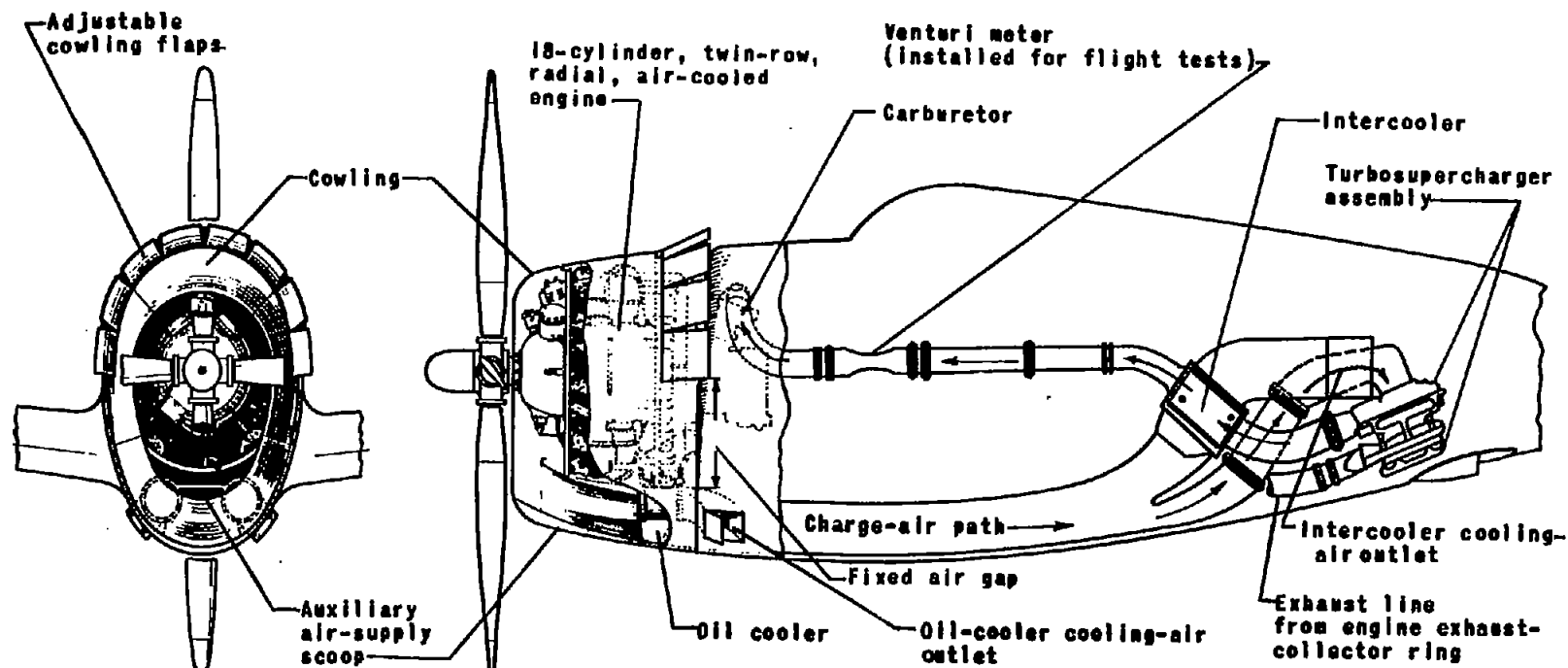
Figure 2. - Power-plant installation in the test airplane.

NATIONAL ADVISORY
COMMITTEE FOR AERONAUTICS

Fig. 2

Fig. 3

P3

H3

P1

P4

H1

H4

H2
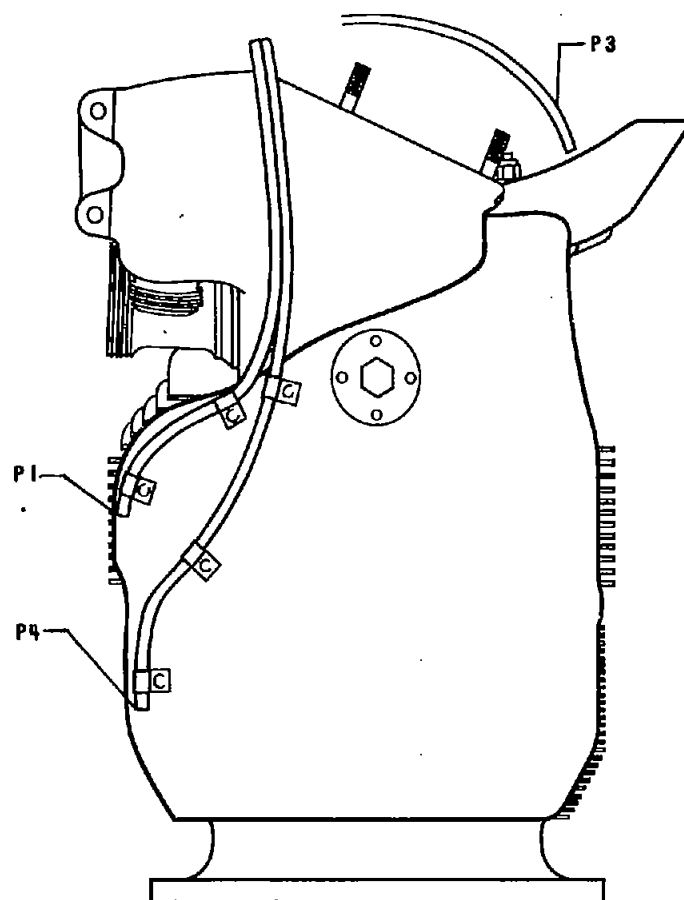
Intake-side view of
rear-row cylinder showing
static-pressure tube
locations

Front view of front-row
cylinder showing total-
head tube locations

NATIONAL ADVISORY
COMMITTEE FOR AERONAUTICS
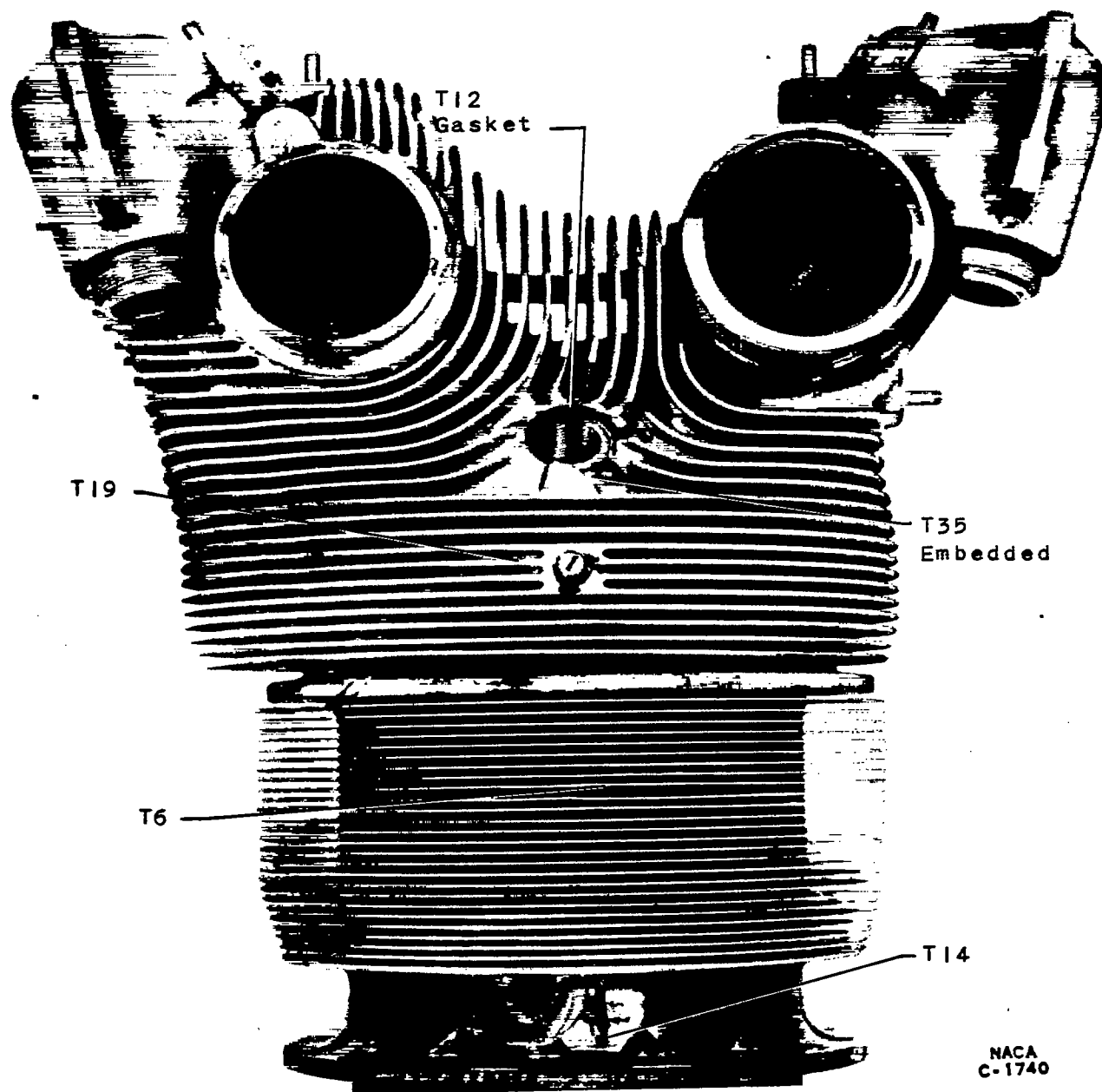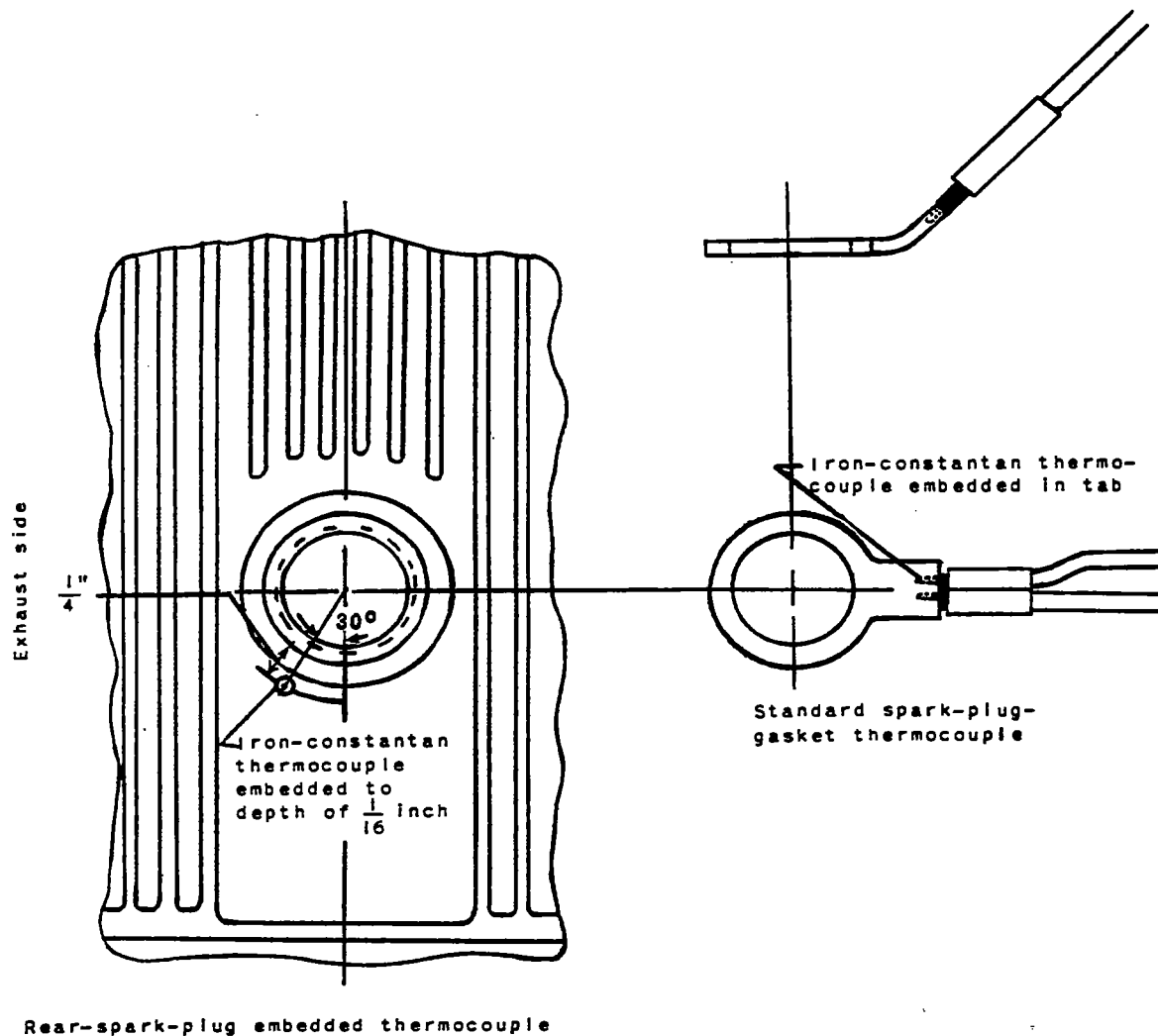
Figure 3. - Cylinder total-head and static-pressure tube locations.

Fig. 4

Figure 4. — Cylinder thermocouple locations.

Fig. 5

Exhaust side

$\frac{1}{4}$"

30°

Iron-constantan
thermocouple
embedded to
depth of $\frac{1}{16}$ inch

Rear-spark-plug embedded thermocouple

Iron-constantan thermo-
couple embedded in tab

Standard spark-plug-
gasket thermocouple

Figure 5. - Details of the rear-spark-plug-boss and gasket
thermocouples.

Fig. 6

NACA TN No. 1089
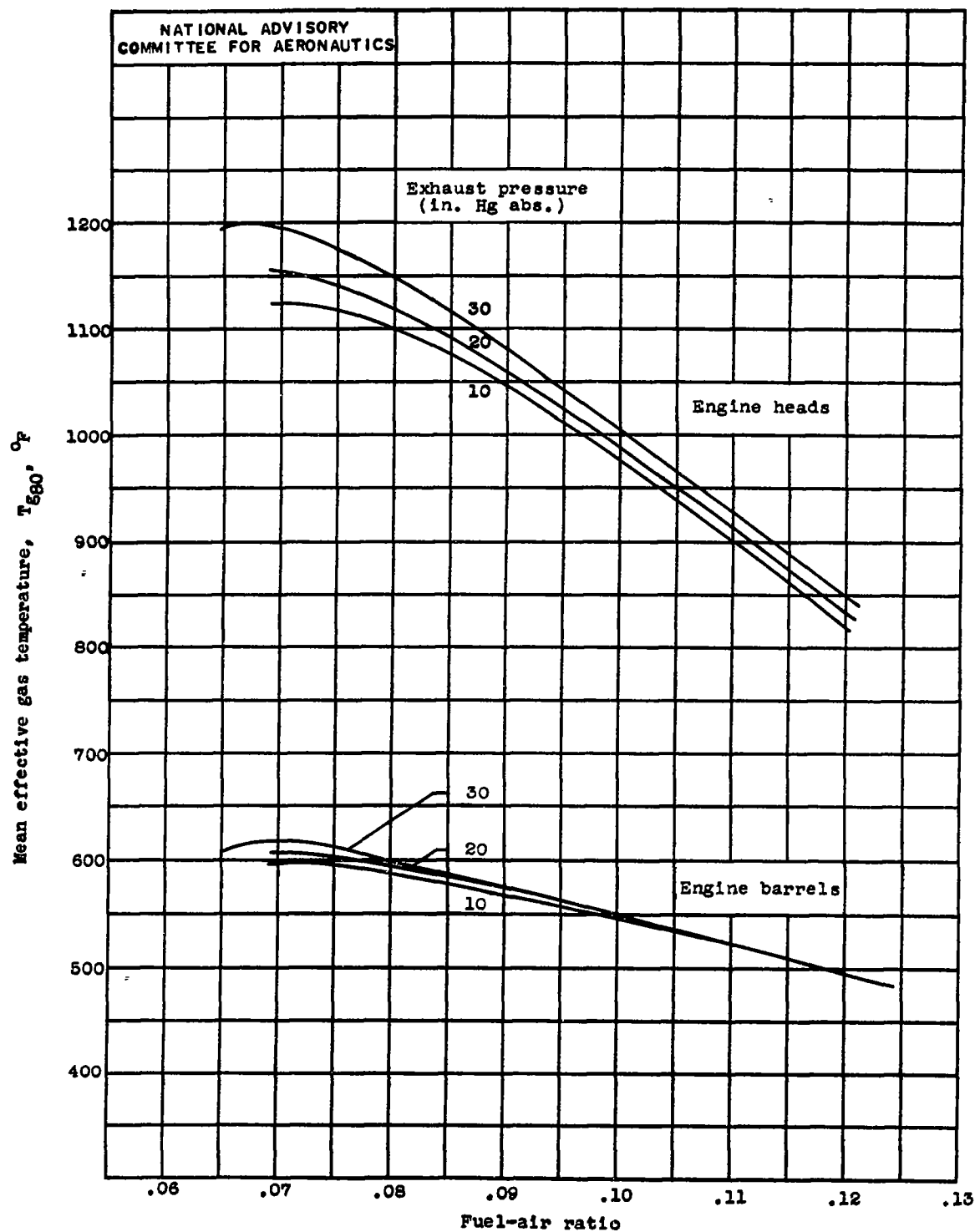
Figure 6.- Variation of mean effective gas temperature with fuel-air ratio and exhaust pressure.

NATIONAL ADVISORY
COMMITTEE FOR AERONAUTICS

	Engine power (bhp)	Average charge-air flow (lb/sec)
O	800	1.73
+	1000	2.06
□	1300	2.95
◇	1500	3.29
△	1100	2.22

$\dfrac{T_h - T_a}{T_g - T_h}$

Slope, -0.35

Cooling-air pressure drop, $\sigma_{en}\Delta p$, in. water

$\dfrac{T_b - T_a}{T_g - T_b}$

Slope, -0.43

Cooling-air pressure drop, $\sigma_{en}\Delta p$, in. water
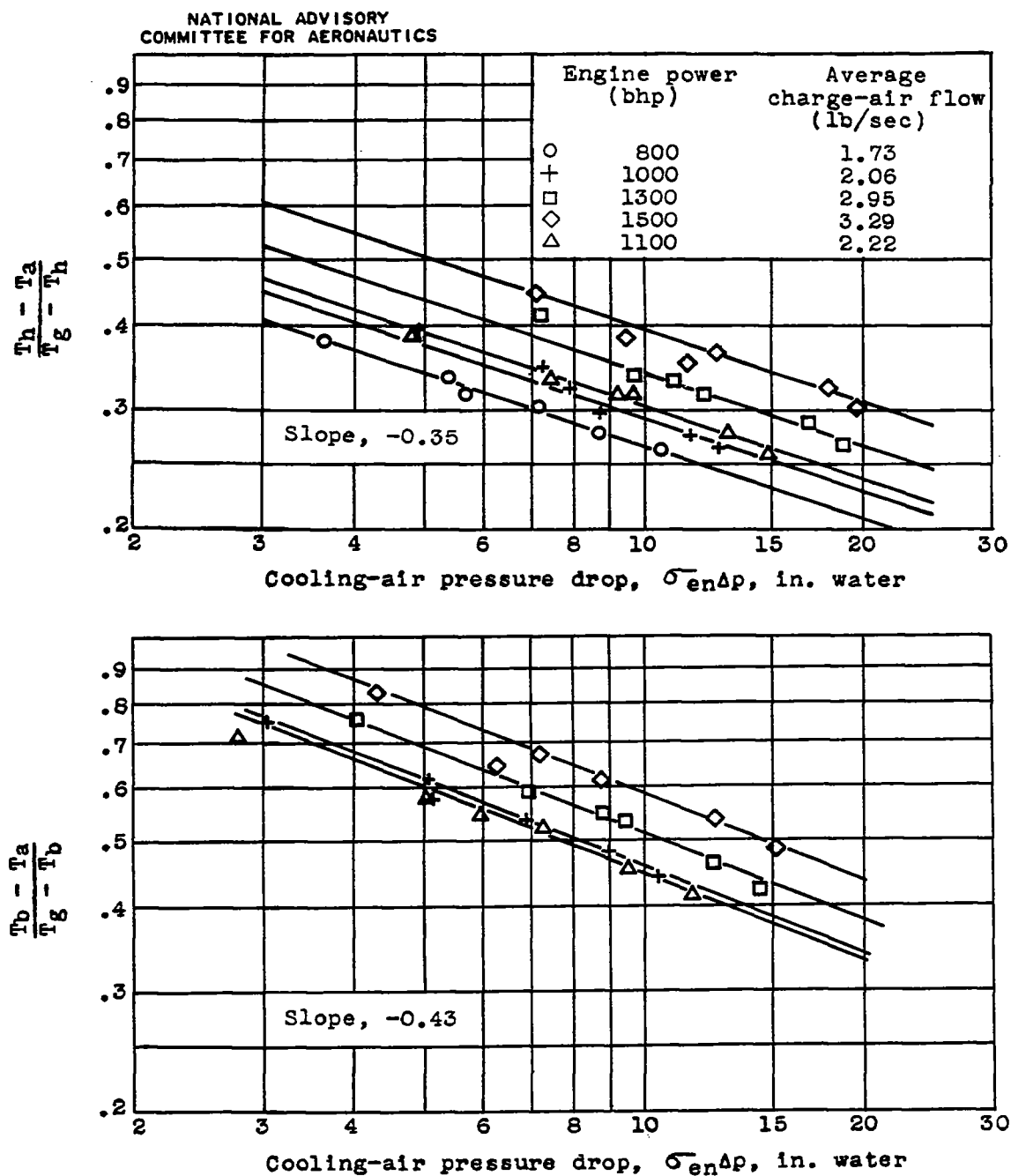
Figure 7. – Variation of $\dfrac{T_h - T_a}{T_g - T_h}$ and $\dfrac{T_b - T_a}{T_g - T_b}$ with cooling-air pressure drop $\sigma_{en}\Delta p$ for various constant charge-air flows at altitude of 5000 feet.

Fig. 8   NACA TN No. 1089
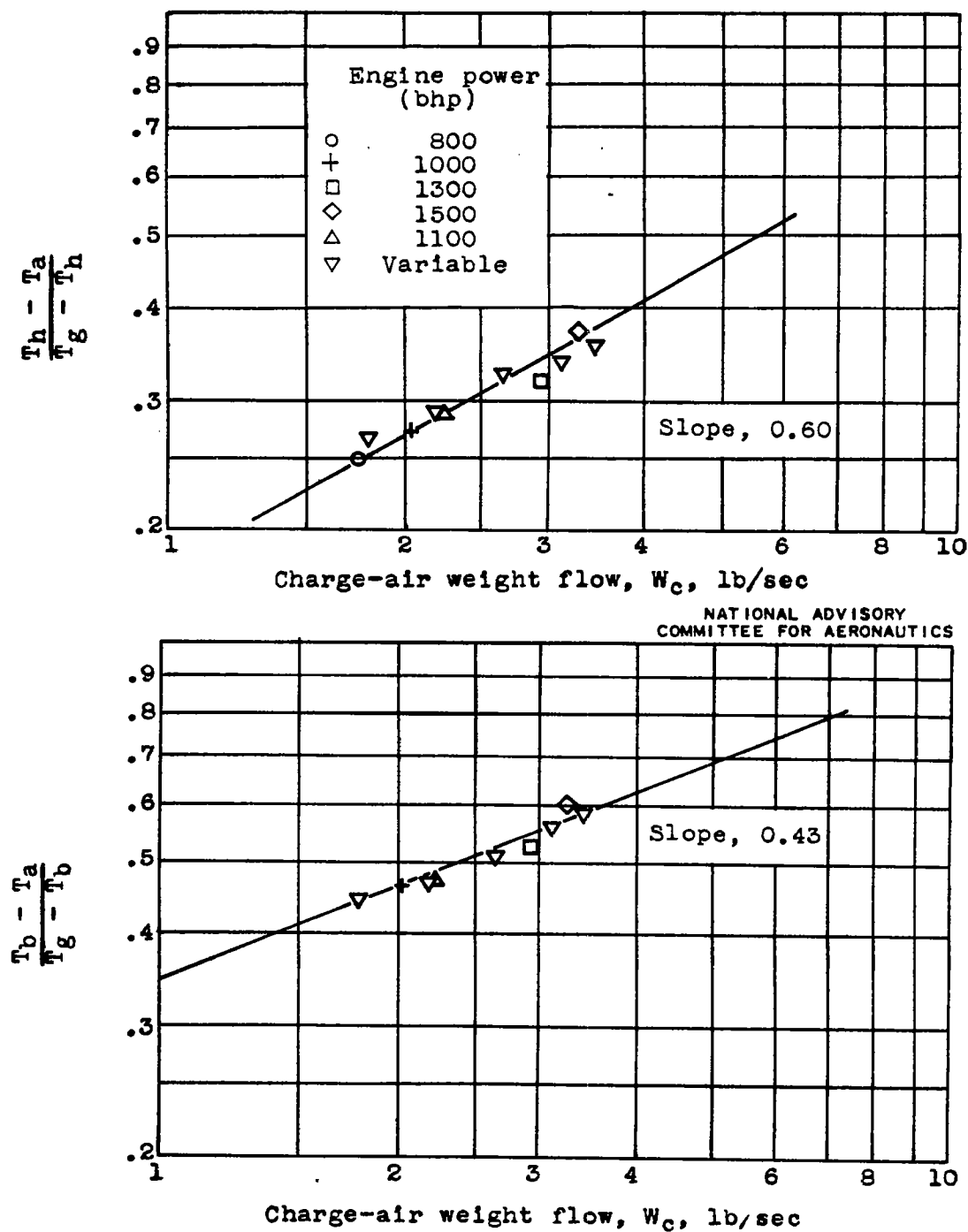
Figure 8.— Variation of $\dfrac{T_h - T_a}{T_g - T_h}$ and $\dfrac{T_b - T_a}{T_g - T_b}$ with charge-air weight flow W_c at constant cooling-air pressure drop of 12 and 9 inches of water for heads and barrels, respectively, at altitude of 5000 feet.
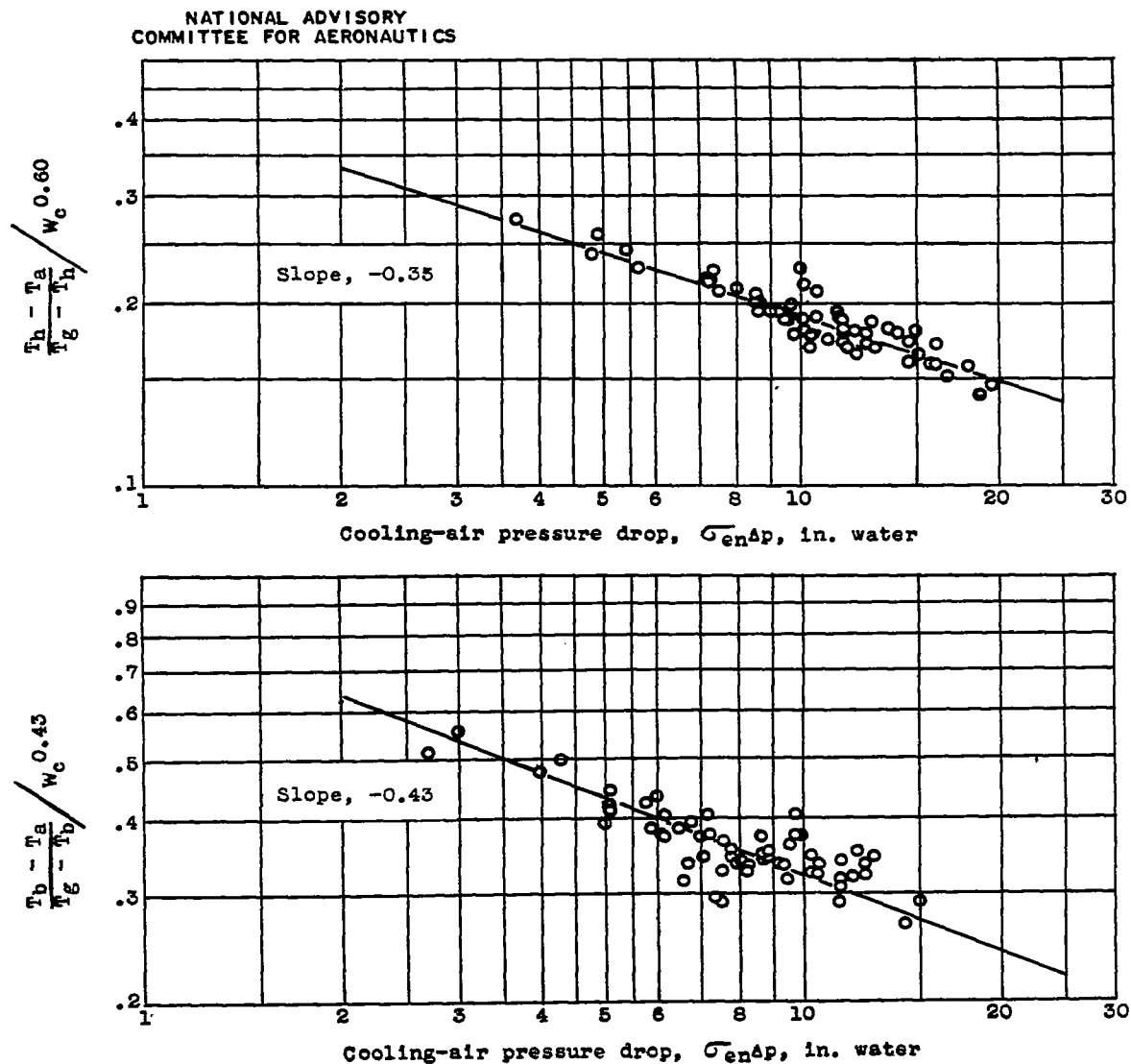
Figure 9. — Cooling-correlation curves based on entrance density for engine heads and barrels at altitude of 5000 feet.
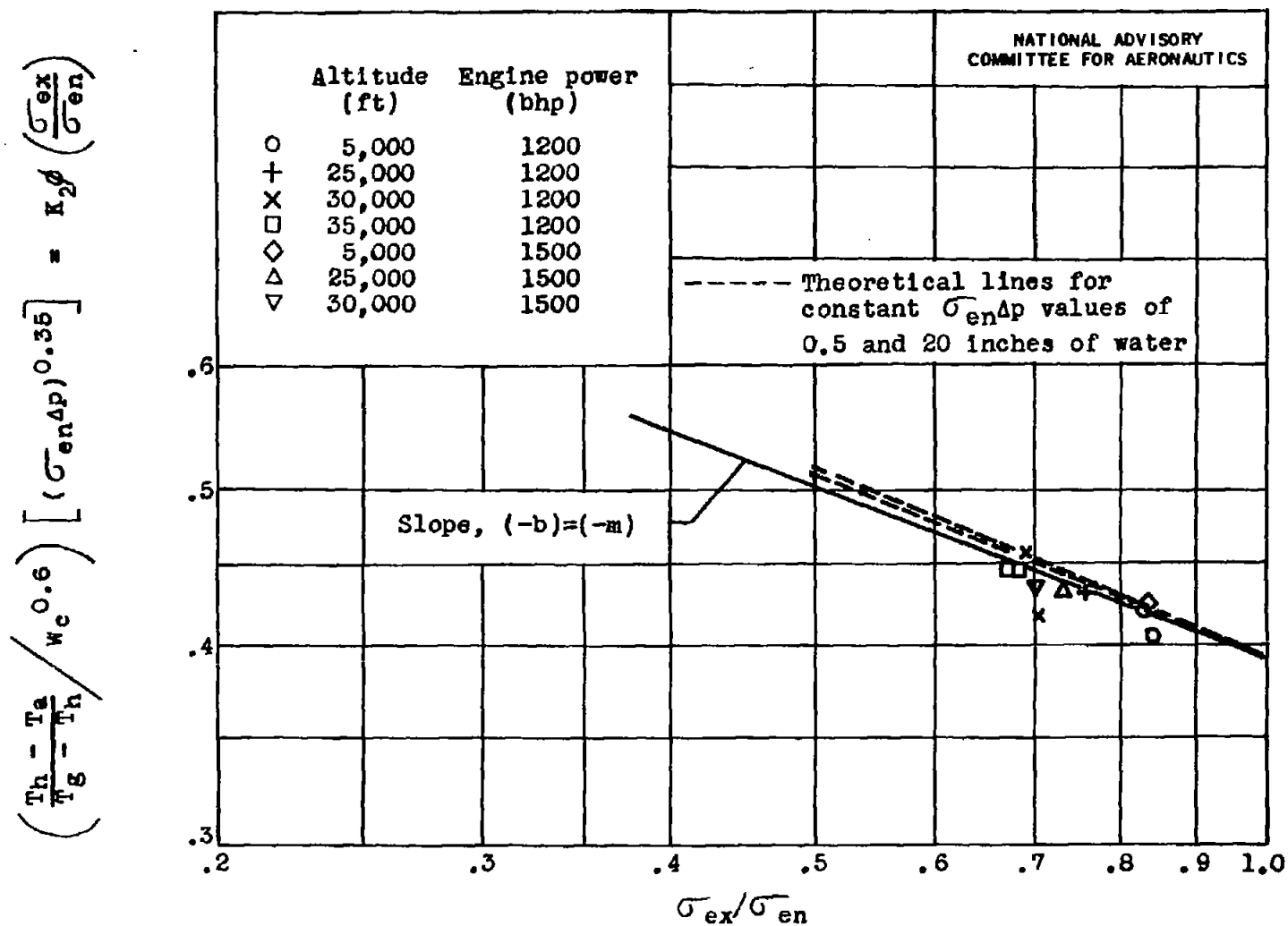
Fig. 10

$$\left(\frac{T_h - T_a}{T_g - T_h} \middle/ w_c^{0.6}\right)\left[(\sigma_{en}\Delta p)^{0.35}\right] = K_2\phi\left(\frac{\sigma_{ex}}{\sigma_{en}}\right)$$

NATIONAL ADVISORY
COMMITTEE FOR AERONAUTICS

	Altitude (ft)	Engine power (bhp)
O	5,000	1200
+	25,000	1200
X	30,000	1200
□	35,000	1200
◇	5,000	1500
△	25,000	1500
▽	30,000	1500

– – – – Theoretical lines for
constant $\sigma_{en}\Delta p$ values of
0.5 and 20 inches of water

Slope, (-b)=(-m)

.6

.5

.4

.3

.2   .3   .4   .5   .6   .7   .8   .9   1.0

σ_{ex}/σ_{en}

Figure 10.- Test variation of the compressibility function $\phi\left(\frac{\sigma_{ex}}{\sigma_{en}}\right)$ with σ_{ex}/σ_{en}
and comparison with theoretically determined variation.
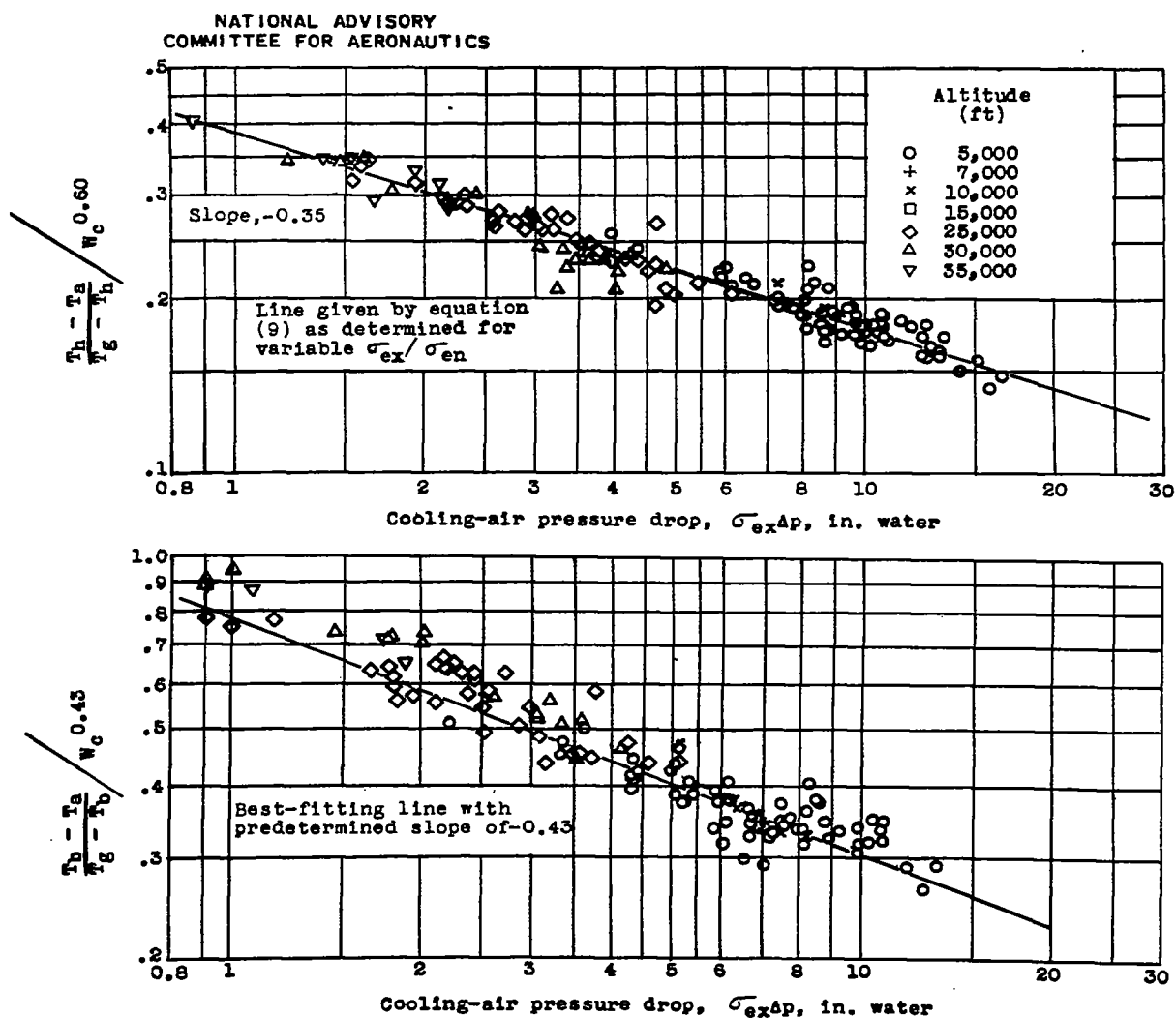
Figure 11.- Cooling-correlation curves based on exit density for engine heads and barrels for altitudes from 5000 to 35,000 feet.

Fig. 12   NACA TN No. 1089
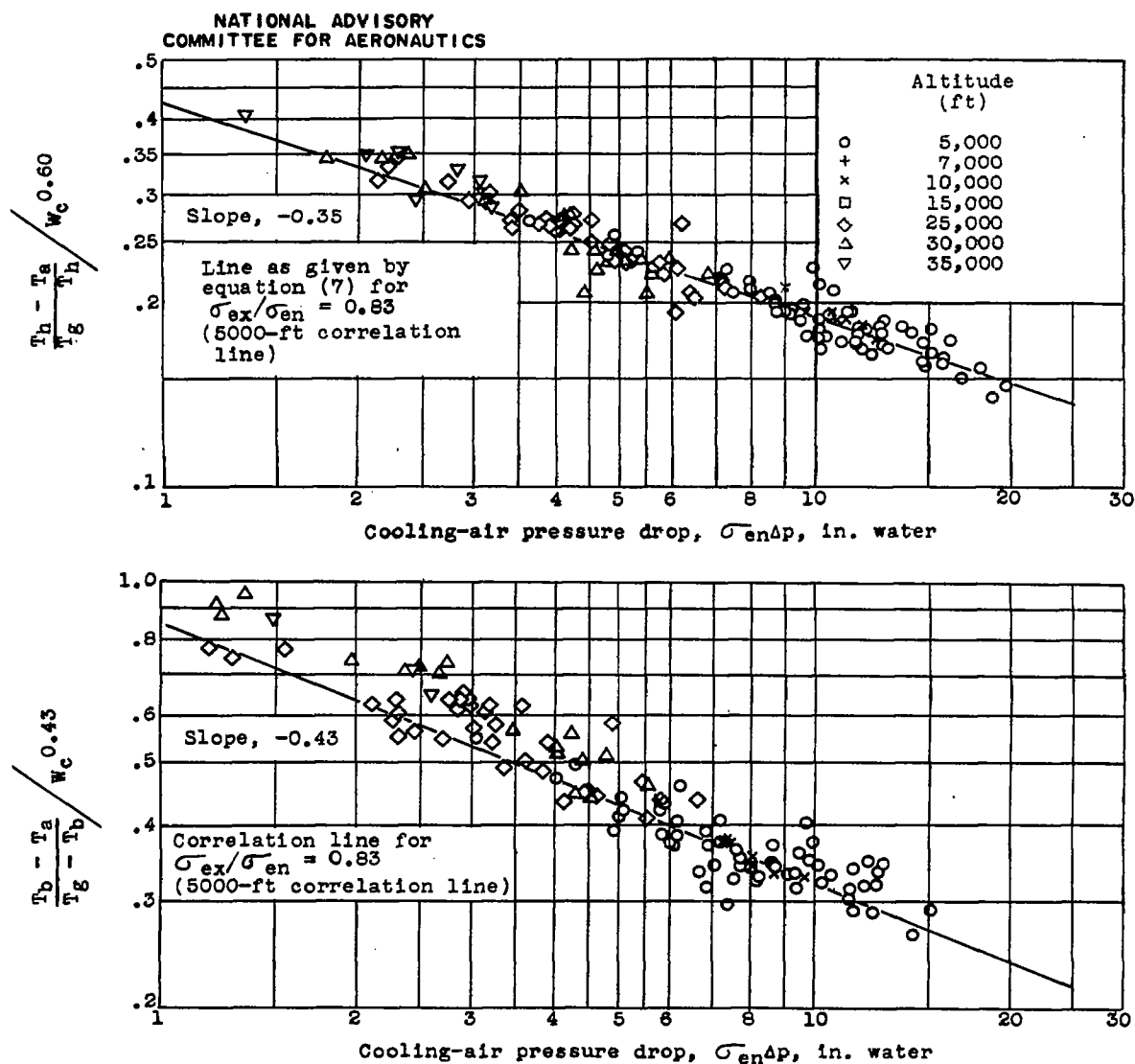
Figure 12.- Cooling-correlation curves based on entrance density for engine heads and barrels for altitudes from 5000 to 35,000 feet.
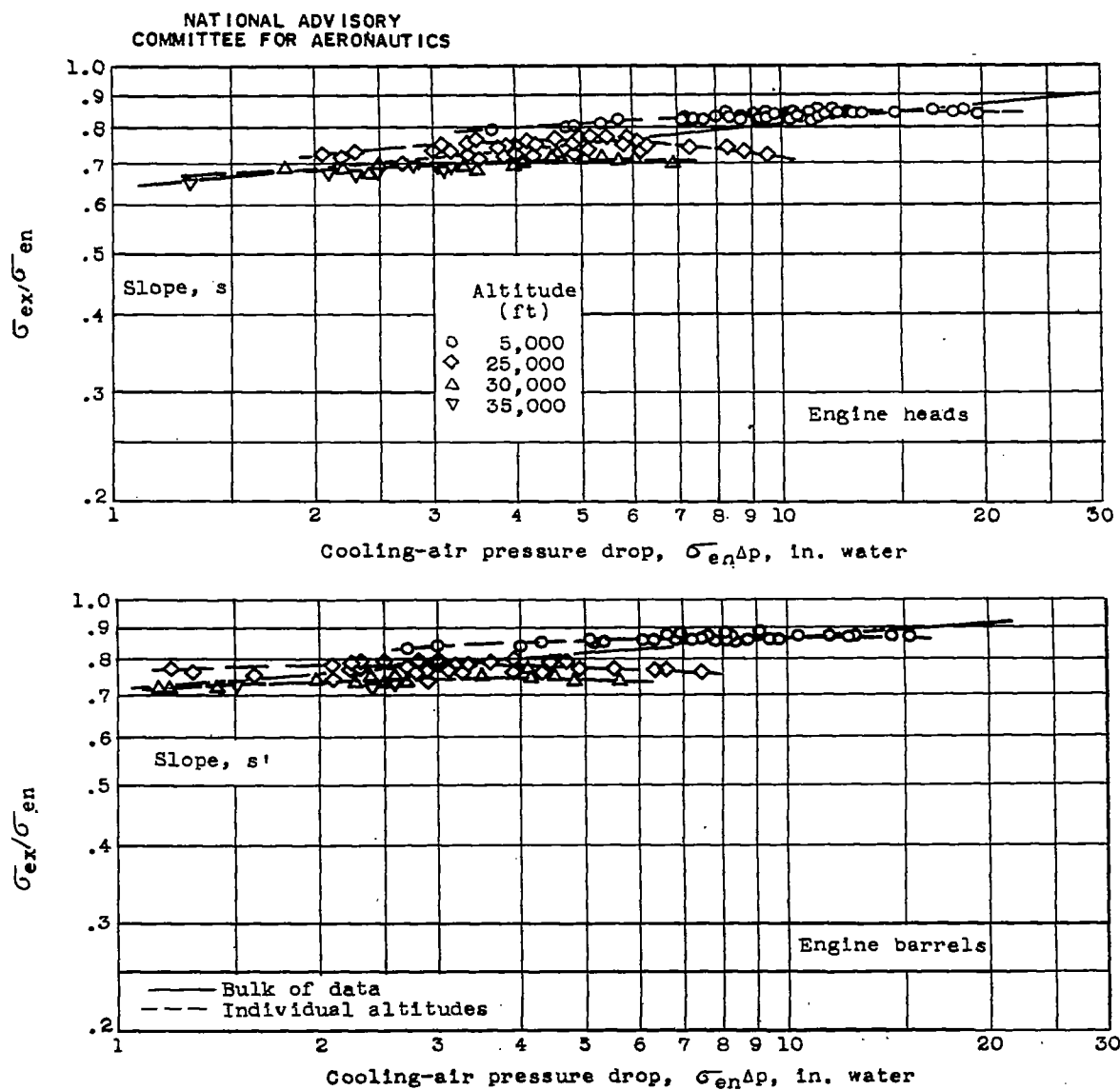
Figure 13.- Variation of σ_{ex}/σ_{en} with cooling-air pressure drop $\sigma_{en}\Delta p$ at altitudes from 5000 to 35,000 feet for engine heads and barrels.
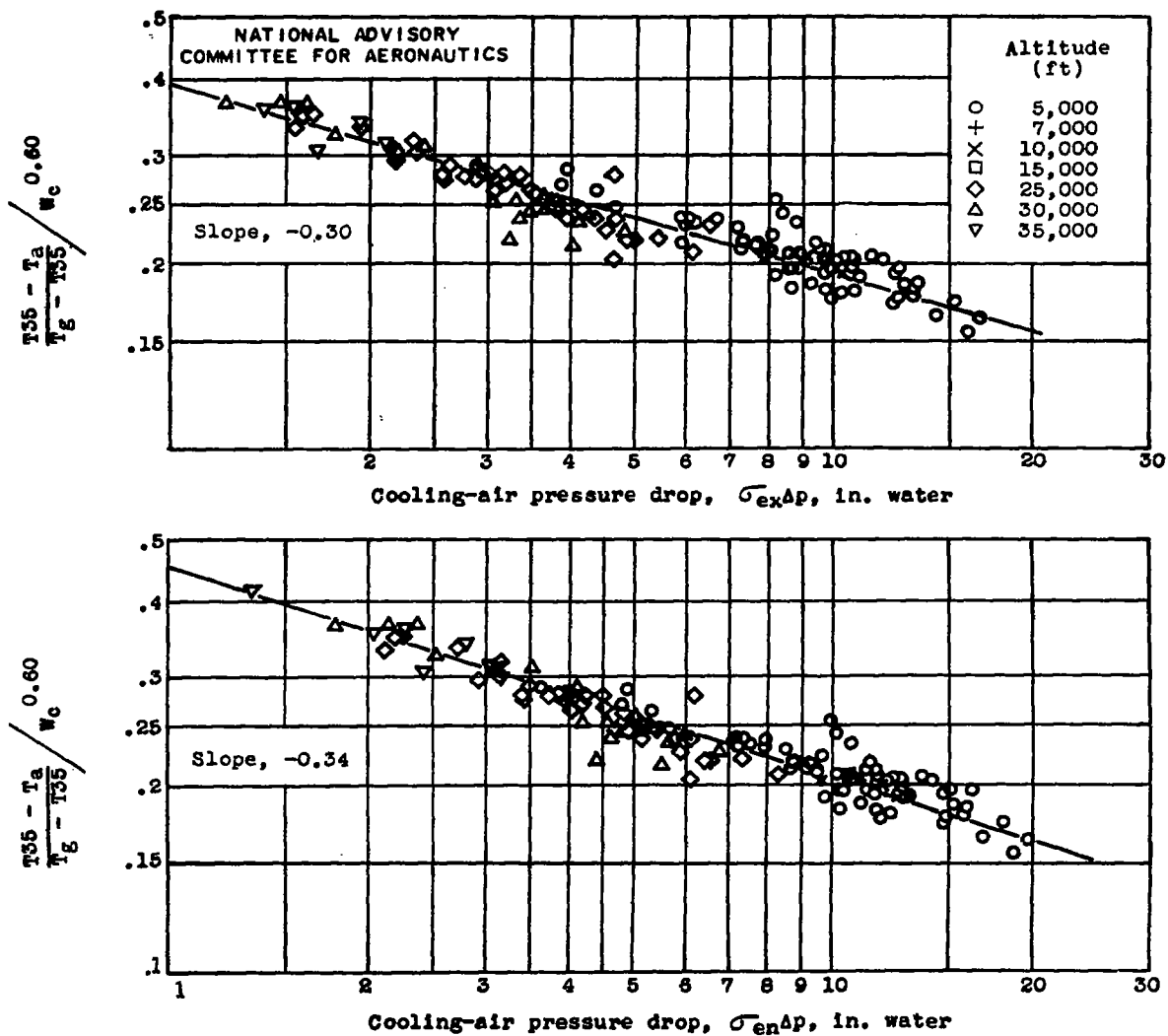
Fig. 14   NACA TN No. 1089

Figure 14. — Cooling-correlation curves based on rear-spark-plug-boss embedded thermo-couples for exit and entrance density for altitudes from 5000 to 35,000 feet. (Curves drawn to best fit all data.)
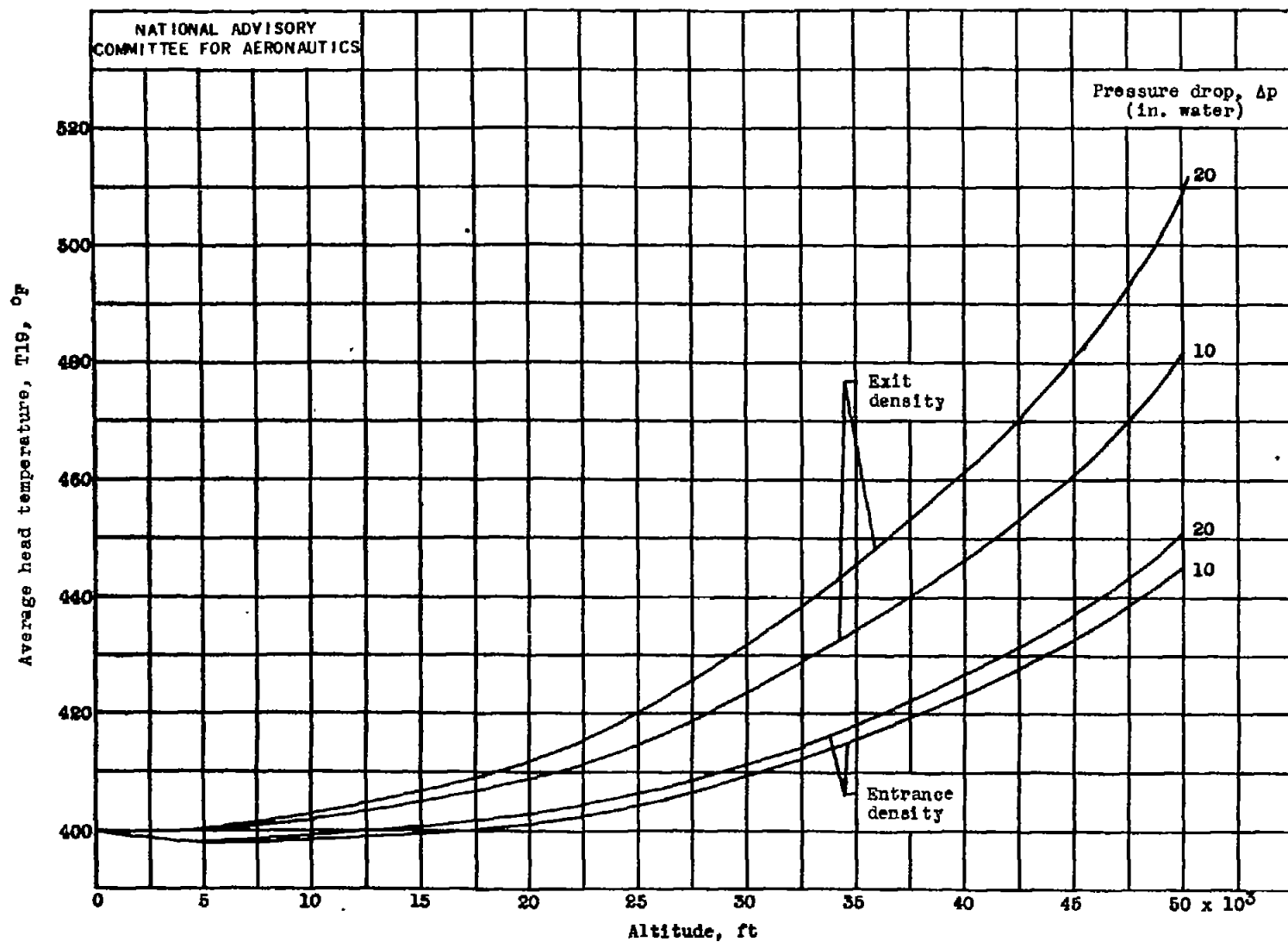
Fig. 15
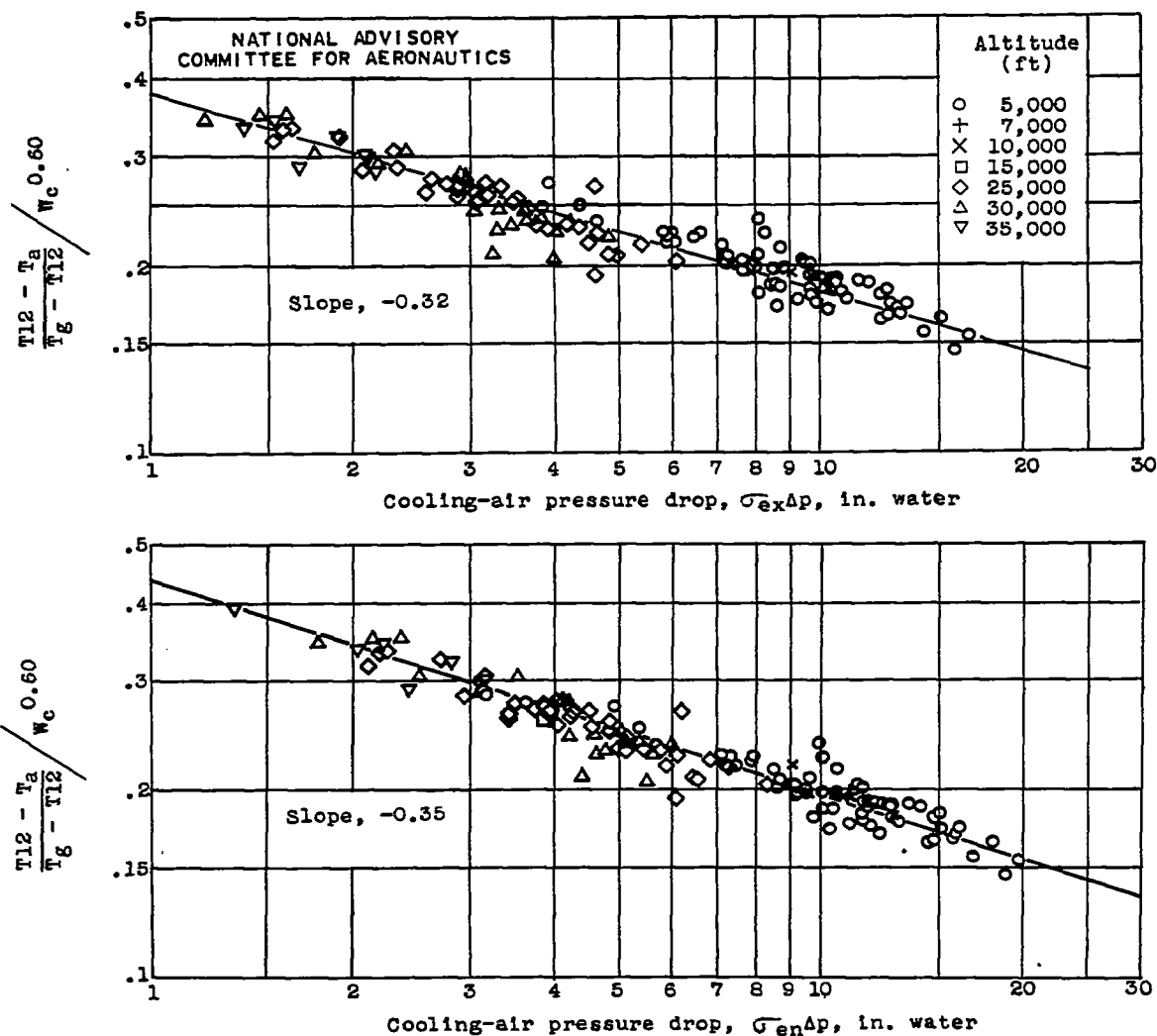
Figure 15. — Cooling-correlation curves based on rear-spark-plug-gasket thermocouples for exit and entrance density for altitudes from 5000 to 35,000 feet. (Curves drawn to best fit all data.)

Fig. 16

Figure 16. - Calculated variation in average head temperature with altitude based on both entrance and exit density for pressure drops of 10 and 20 inches of water. Engine power, 1625 brake horsepower; engine speed, 2400 rpm; charge-air weight flow, 3.5 pounds per second; Army summer air.
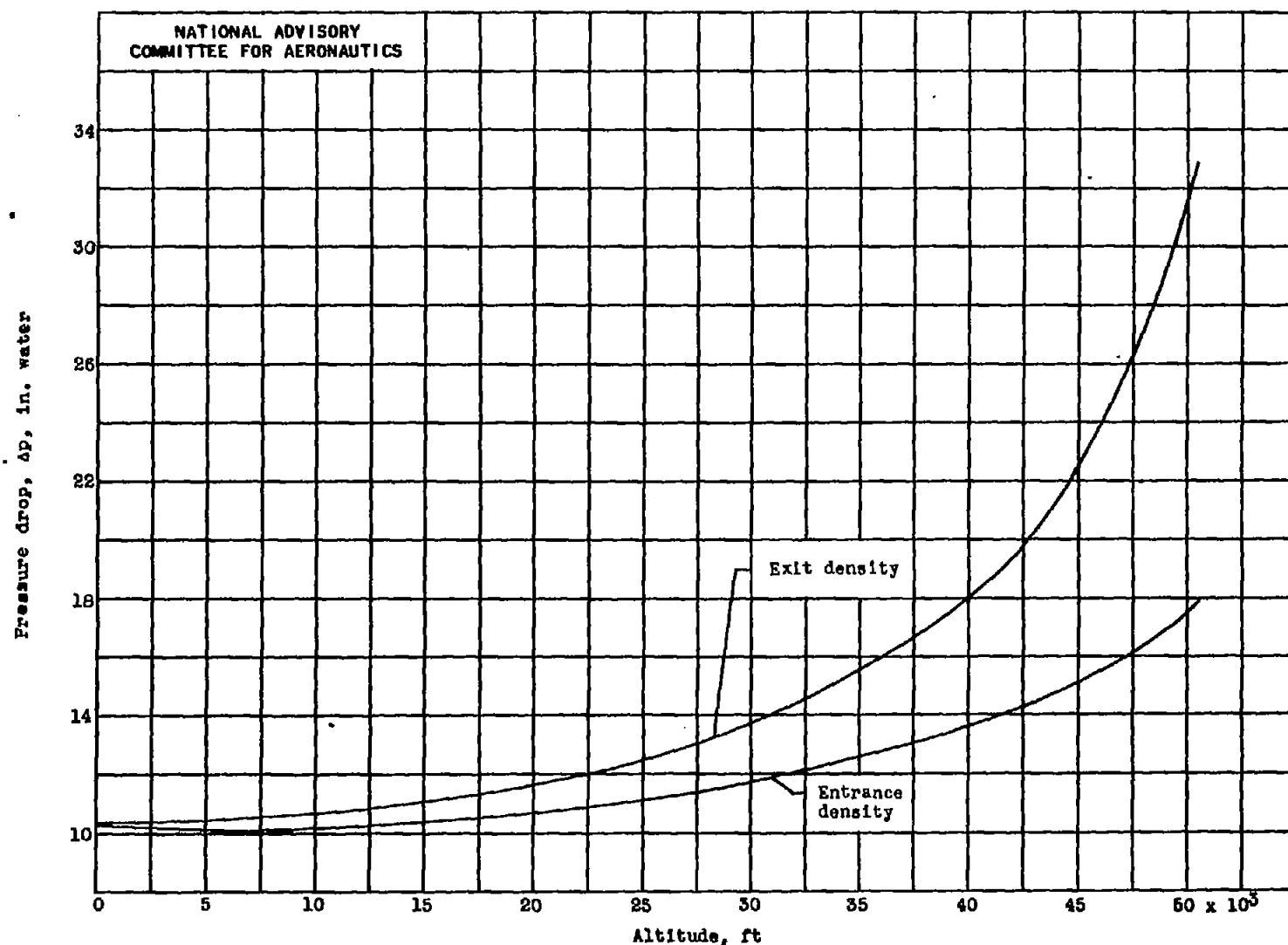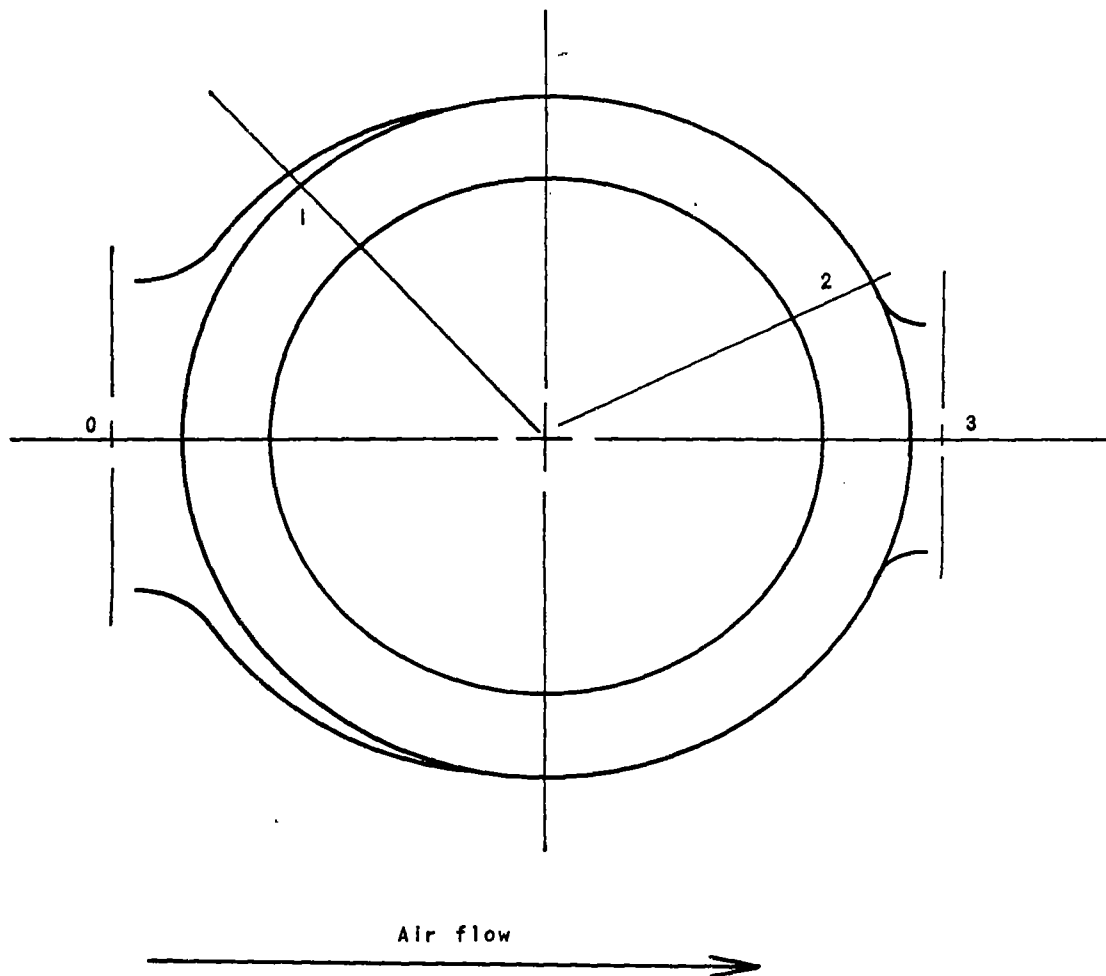
Fig. 17

Figure 17. – Calculated variation of pressure drop with altitude necessary to maintain constant head temperature T19. Engine power, 1625 brake porsepower; engine speed, 2400 rpm; charge-air weight flow, 3.5 pounds per second; fuel-air ratio, 0.10; Army summer air.

Fig. 18   NACA TN No. 1089

Air flow

Figure 18. — Diagram of cooling-air flow path across an
engine cylinder.
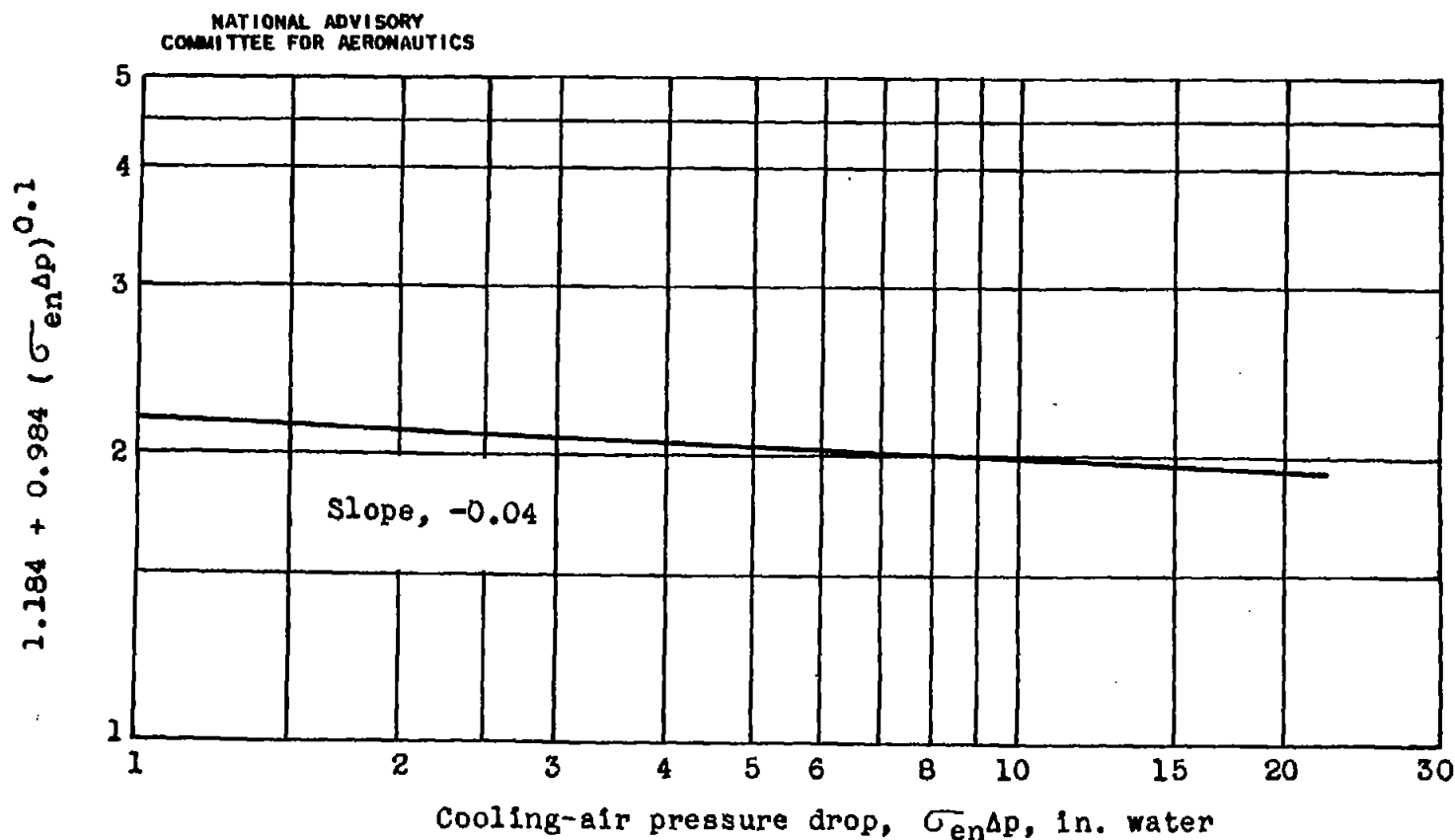
Figure 19.- Plot for evaluation of parameters r and $\frac{K_1}{k}$ of equation (22).

Fig. 19

Fig. 20   NACA TN No. 1089
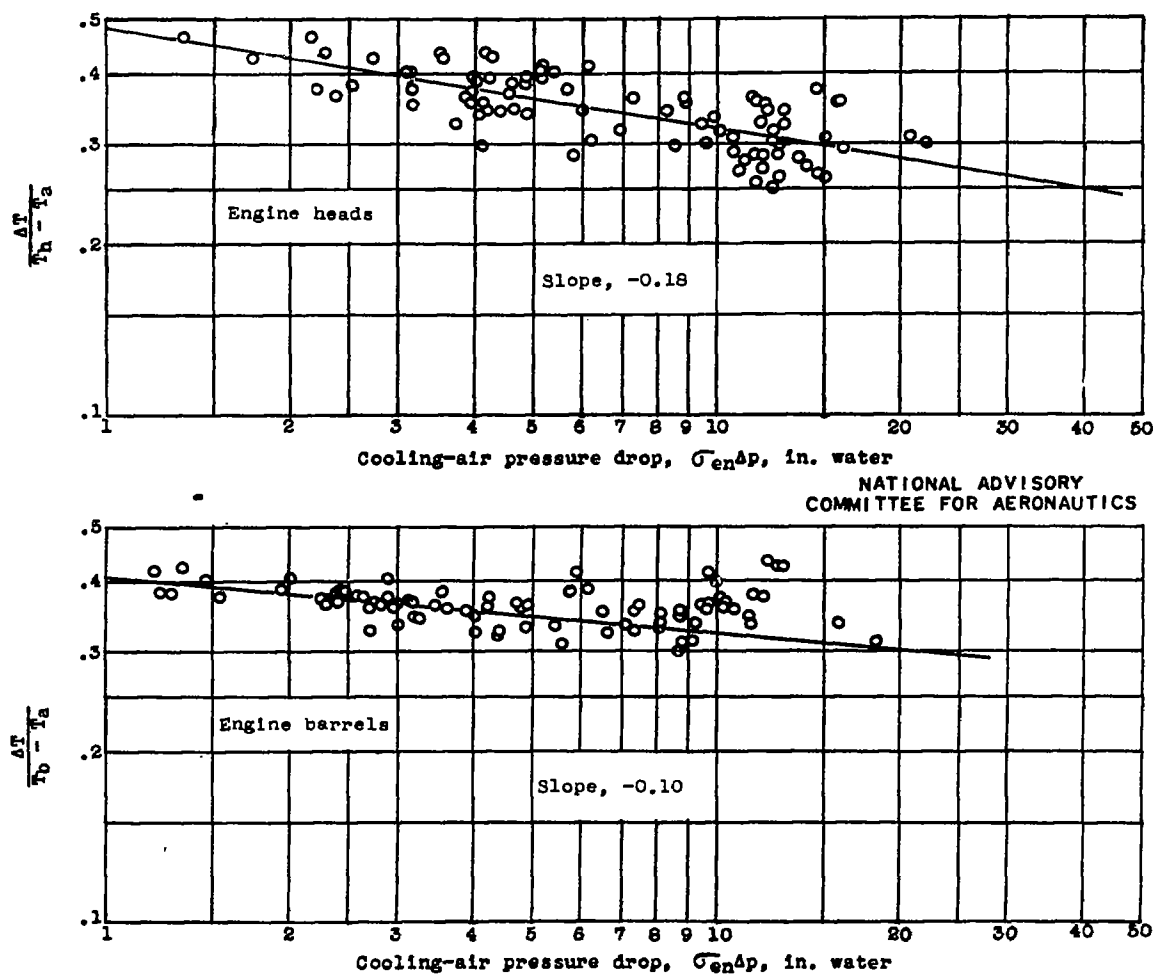

Figure 20.- Variation in cooling-air temperature rise parameter with cooling-air pressure drop $\sigma_{en}\Delta p$ for engine heads and barrels.